SPACE, TELECOMMUNICATIONS AND RADIOSCIENCE LABORATORY

STARLAB
DEPARTMENT OF ELECTRICAL ENGINEERING / SEL
STANFORD UNIVERSITY • STANFORD, CA 94305

# AN AUTOMATIC REAL-TIME GEOMAGNETIC ACTIVITY MONITORING SYSTEM FOR THE MAD AND ADJACENT FREQUENCY BANDS

by
A. Bernardi
A.C. Fraser-Smith
O.G. Villard, Jr.

Final Technical Report E724-2

November 1988



Sponsored by
The Office of Naval Research
through
Contract No. N00014-83-K-0390

# REPORT DOCUMENTATION PAGE

| | |
|---|---|
| 1a. REPORT SECURITY CLASSIFICATION: Unclassified | 1b. RESTRICTIVE MARKINGS: N/A |
| 2a. SECURITY CLASSIFICATION AUTHORITY: N/A | 3. DISTRIBUTION/AVAILABILITY OF REPORT: Approved for public release: distribution unlimited |
| 2b. DECLASSIFICATION/DOWNGRADING SCHEDULE: N/A | |
| 4. PERFORMING ORGANIZATION REPORT NUMBER(S): E724-2 | 5. MONITORING ORGANIZATION REPORT NUMBER(S) |
| 6a. NAME OF PERFORMING ORGANIZATION: STAR Laboratory; 6b. OFFICE SYMBOL (If applicable) | 7a. NAME OF MONITORING ORGANIZATION |
| 6c. ADDRESS (City, State and ZIP Code): Stanford University, Stanford, CA 94305 | 7b. ADDRESS (City, State and ZIP Code) |
| 8a. NAME OF FUNDING/SPONSORING ORGANIZATION: Office of Naval Research; 8b. OFFICE SYMBOL (If applicable) | 9. PROCUREMENT INSTRUMENT IDENTIFICATION NUMBER: Contract No. N00014-83-K-0390 |
| 8c. ADDRESS (City, State and ZIP Code): 800 N. Quincy Street, Code 1114SP, Arlington, VA 22217 | 10. SOURCE OF FUNDING NOS: PROGRAM ELEMENT NO. 61153N; PROJECT NO. 4149; TASK NO. 168; WORK UNIT NO. |
| 11. TITLE (Include Security Classification) | |

12. PERSONAL AUTHOR(S): A. Bernardi, A.C. Fraser-Smith, O.G. Villard, Jr.

| 13a. TYPE OF REPORT | 13b. TIME COVERED | 14. DATE OF REPORT (Yr., Mo., Day) | 15. PAGE COUNT |
|---|---|---|---|
| FINAL | FROM 5/15/83 TO 9/30/88 | 1988 Nov. | 59 |

16. SUPPLEMENTARY NOTATION

| 17. COSATI CODES | | | 18. SUBJECT TERMS (Continue on reverse if necessary and identify by block number) |
|---|---|---|---|
| FIELD | GROUP | SUB GR | MAD, Geomagnetic Activity, ULF Submarine Detection, Remote Measurement Systems |
| | | | |

19. ABSTRACT (Continue on reverse if necessary and identify by block number)
A digital signal processing system for the measurement and monitoring of fluctuations of the Earth's magnetic field with frequencies in the range 0.01-10 Hz, i.e., predominantly in the ultra-low frequency range (ULF; f ≤ 5 Hz), is described. The system was designed and developed at Stanford University with support from the Office of Naval Research. It operates automatically under the control of a small computer and it generates indices by computing the logarithm of the average power in the frequency bands of interest, including in particular the band used for magnetic anomaly detection (MAD). The indices are therefore a direct measure of the levels of magnetic activity in their respective frequency bands. Two such systems were operated in the U.S., one on the East Coast (geomagnetic latitude 55°N) and the other on the West Coast (geomagnetic latitude 43°N). Real-time information on the levels of magnetic activity in the bands monitored by either of the systems was accessible from anywhere in the U.S. at any time via telephone line. The automatic operation of these systems, combined with a diagnostic/calibration capability that could be activated over the telephone line, (continued)

| | |
|---|---|
| 20. DISTRIBUTION/AVAILABILITY OF ABSTRACT: UNCLASSIFIED/UNLIMITED ☐ SAME AS RPT. ☒ DTIC USERS ☐ | 21. ABSTRACT SECURITY CLASSIFICATION: UNCLASSIFIED |
| 22a. NAME OF RESPONSIBLE INDIVIDUAL | 22b. TELEPHONE NUMBER (Include Area Code); 22c. OFFICE SYMBOL |

FORM 1473, 83 APR EDITION OF 1 JAN 73 IS OBSOLETE.

allowed them to operate unattended for many months.

As shown by illustrative examples, the indices on the East Coast are usually substantially larger, and have a greater variation, than those on the West Coast, a difference which we ascribe to the greater geomagnetic latitude of the ~~East Coast~~ measurement site. Some of the indices, including some of those for the MAD band, have a well defined diurnal variation, whereas others have little or no such variation. In the MAD band, the East Coast indices can vary by 20 dB or more in a single day, illustrating the desirability of active monitoring. Our interpretation of the measurements suggests that the diurnal and other variations could be even larger at higher latitudes. There is little correlation between time variations of our indices and variations of the standard three-hour range index Kp, and there is of course no diurnal variation in the latter index to match those in some of our indices, since Kp was intended to be a planetary index and it is constructed in such a way that it has essentially no 24-hr variation. ~~We find that~~ linear prediction techniques can be used effectively to predict our indices for up to 24 hours ahead. It should therefore be possible to anticipate the level of natural noise that will be encountered in the MAD band for up to a day before an MAD mission.

# An Automatic Real-Time Geomagnetic Activity Monitoring System for the MAD and Adjacent Frequency Bands

A. Bernardi
A. C. Fraser-Smith
O. G. Villard, Jr.

*STAR Laboratory*
*Department of Electrical Engineering, Stanford University*
*Stanford, California, 94305*

Final Technical Report E724-2

November 1988

Sponsored by
The Office of Naval Research
through
Contract No. N00014-83-K-0390

# Contents

# List of Figures



# List of Tables

# Abstract

A digital signal processing system for the measurement and monitoring of fluctuations of the Earth's magnetic field with frequencies in the range 0.01–10 Hz, i.e., predominantly in the ultra-low frequency range (ULF; $f \lesssim 5$ Hz), is described. The system was designed and developed at Stanford University with support from the Office of Naval Research. It operates automatically under the control of a small computer and it generates indices by computing the logarithm of the average power in the frequency bands of interest, including in particular the band used for magnetic anomaly detection (MAD). The indices are therefore a direct measure of the levels of magnetic activity in their respective frequency bands. Two such systems were operated in the U.S., one on the East Coast (geomagnetic latitude 55° N) and the other on the West Coast (geomagnetic latitude 43° N). Real-time information on the levels of magnetic activity in the bands monitored by either of the systems was accessible from anywhere in the U.S. at any time via telephone line. The automatic operation of these systems, combined with a diagnostic/calibration capability that could be activated over the telephone line, allowed them to operate unattended for many months.

As shown by illustrative examples, the indices on the East Coast are usually substantially larger, and have a greater variation, than those on the West Coast, a difference which we ascribe to the greater geomagnetic latitude of the East Coast measurement site. Some of the indices, including some of those for the MAD band, have a well defined diurnal variation, whereas others have little or no such variation. In the MAD band, the East Coast indices can vary by 20 dB or more in a single day, illustrating the desirability of active monitoring. Our interpretation of the measurements suggests that the diurnal and other variations could be even larger at higher latitudes. There is little correlation between time variations of our indices and variations of the standard three-hour range index $Kp$, and there is of course no 'diurnal' variation in the latter index to match those in some of our indices, since $Kp$ was intended to be a planetary index and it is constructed in such a way that it has essentially no 24-hr variation. We find that linear prediction techniques can be used effectively to predict our indices for up to 24 hours ahead. It should therefore be possible to anticipate the level of natural noise that will be encountered in the MAD band for up to a day before an MAD mission.

# Acknowledgments

This work was sponsored by The Office of Naval Research through Contract No. N00014-83-K-0390. We would like to thank Paul McGill for the help and technical advice given during the design and development of the systems. We also thank Dr. Alan Phillips for his help in design of the low noise amplifiers, and Prof. Otto Heinz of the Naval Postgraduate School, both for his early participation in this project and for making available the site at which the first MA Index Generation System was operated.

Finally, we would like to thank the people who have provided the low-noise sites where our two final systems were operated. For the West Coast site we would like to thank Kathy, Kirk, and Katie Mathew, and for the East Coast site we thank Mike Trimpi. We also appreciate the technical assistance provided by Mike Trimpi.

# Summary

This report details the results of a project, begun at Stanford in 1981, to improve the U.S. Navy's Magnetic Anomaly Detection (MAD) capability by providing better information about the state of natural geomagnetic activity in the frequency range used for MAD.

At present, the Navy uses three indices, $Kp$, $Ap$, and $A_{FT}$, to provide information about the level of geomagnetic activity in the MAD band. This use can only be justified by the current lack of better indicators, for, while there can be correspondences on occasion between increases in the above indices and increases in natural activity in the MAD band, the indices were never intended to be indicators of MAD-band activity and on many occasions they provide no reliable indication of the state of natural activity in the band. In fact, as we show in this report, they can provide misleading information. The indices also have other defects from the point of view of the Navy's need. In particular, they provide little information about the diurnal variation of MAD-band activity, which can sometimes amount to about 20 dB or more at higher latitudes, and they give no reliable information about the level of geomagnetic activity at high latitudes, which can be much greater than the level at middle and low latitudes. This latter point is of particular concern, because the northern high latitudes include ocean areas of great importance to the Navy.

In response to this problem, we have designed, constructed, tested, and deployed two operating versions of a geomagnetic activity measurement system that runs under the control of a small computer and which automatically derives half-hour indices of geomagnetic activity for nine non-overlapping frequency bands covering the range 0.01–10 Hz. The indices for these bands provide important diagnostic information about the predominantly ultra-low-frequency (ULF; frequencies less than 5 Hz) activity occurring in and around the MAD range. In addition, half-hour indices are also derived for three frequency bands specific to the MAD frequency range; one band covers a commonly used band for MAD operations (0.04–0.60 Hz), and the other two cover the upper (0.20–2.00 Hz) and lower (0.04–0.20 Hz) parts of the nominal overall MAD range (0.04–2.00 Hz).

Unlike the $K$ and $A$ range indices, our indices provide a direct measure of the average power of the magnetic field fluctuations in the MAD and adjacent frequency bands. They are derived by sampling the output voltage of the solenoid field sensor at a 30 $s^{-1}$ rate, frequency analyzing the data in blocks of 4096 samples (136 s of data), and averaging 13 or 14 of the resulting power spectrums to get an average half-hour power spectrum. The individual indices are then obtained by taking the logarithm to the base two of the average power in the appropriate frequency bands. This index generation process is clearly very flexible and the time interval covered by the indices can be varied within wide limits; our choice of a half-hour interval was prompted by a desire for greater time resolution than that provided by the $K$ and $A$ indices.

The two MAD index generation systems were deployed on the East and West coasts

of the U.S., one in New Hampshire and the other in California, at relatively remote locations to avoid magnetic noise from man-made sources. The precise locations are not critical, since the systems are designed to have their indices (and other system information) accessed over a telephone line. As a result, the indices were continuously available, under password control, to users anywhere, provided only that they had an appropriate computer terminal, a modem, and access to a telephone line.

Comparison of the East and West coast indices gives interesting results. First, the indices are larger in New Hampshire than they are in California, as would be anticipated due to the higher geomagnetic latitude of the East Coast location (54°35'N) compared with that in California (43°23'N). However, the difference in amplitude can be substantial: for example, the East Coast indices can be up to 6–9 dB greater than those on the West Coast in the 0.05–0.1 Hz frequency band. Second, cross correlations of the two sets of indices show that there are correlations between the activity in the 0.01–0.1 Hz and 5–10 Hz ranges, but there is little or no correlation for the 0.1–5 Hz range. There is an observed time lag in the California data of approximately 3 hours. These results suggest that measurements of MAD indices on one coast could be used to make rough estimates of the activity in the MAD range on the other coast, or, more generally, that only a few MAD index generators would be required to monitor MAD-band activity over large areas. However, our measurements have not included any high-latitude locations, where the natural activity is likely to have a greater spatial variation.

Using a linear prediction filter method, we have investigated the possibility of making predictions of the MAD indices. The method is most accurate for short time intervals, from one half-hour to several hours ahead, but comparatively successful predictions can be made for longer time intervals. In particular, moderately accurate predictions of the indices for 24 hours ahead appear likely to be feasible.

Several evolutionary improvements of the MAD index generators are possible, but even in their present configuration they provide the Navy with a powerful new monitoring capability. The indices can be accessed at any time from a Naval Air Station, or other Navy facility (with telephones), and they provide an accurate measure of natural activity in the MAD range at the locations of the index generators, and over large surrounding areas (the full extent of these areas remains to be established, but a surrounding area of a few thousand square miles at middle latitudes does not appear unreasonable at this time). New indices are computed every half-hour, and the indices currently in preparation are also available in preliminary form at any time, thus providing the user with real-time information. Finally, predictions of the indices for up to 24 hours ahead can also be provided, thus facilitating mission planning. The index generation systems are compact and inexpensive in the form in which we have built them. Since one system is likely to give adequate information about the state of MAD-band activity over a surrounding area of a few thousand square miles, it may be possible to deploy enough systems to give complete coverage of all important regions for Navy MAD operations.

# 1 Introduction

This report describes a signal processing system developed at Stanford University for the study of naturally occurring geomagnetic signals on Earth's surface at frequencies in the range 0.01 Hz to 10.0 Hz. The system will be referred to here as the Magnetic Activity Index (MAI) Generation System, and two such systems were operated, one on the West Coast of the U.S., the MAI-West system, and the other on the East Coast, the MAI-East system.

The primary goal of this work was to develop a new, real-time, capability for studying geomagnetic activity in the above predominantly ULF range over long periods of time, of the order of years. Similar long term studies have not been aimed at these ULF ranges [*Sentman*, 1987]. Other real-time indices of geomagnetic activity have been proposed before [*Joselyn*, 1970], but they lack the frequency resolution needed for our work.

Each MAI Generation System is intended to be operated at a location as far away as possible from ac power line interference and other forms of man made noise that are found in city environments. The artificial magnetic signals encountered in city environments have been discussed before [*Fraser-Smith and Coates*, 1978; *Ho et al.*, 1979; *Samadani et al.*, 1981], and an example of the MAI Generation System response to such signals is presented in Section 5. The geomagnetic data collected by the MAI Generation Systems at our remote sites were further processed at Stanford University to obtain profiles of the magnetic activity at those sites, and they were analyzed to provide information concerning correlations between the data from the two sites. Predictions of magnetic activity were also made, based on the collected data using linear prediction techniques, and these results are reported in Section 9.

From earlier studies of naturally occurring low frequency magnetic signals [*Jacobs*, 1970; *Fraser*, 1975] it was expected that there would be no significant polarization of geomagnetic activity in either the East-West or North-South directions over long periods of time. Thus, the MAI Generation System was designed as a single channel system with an overall frequency range of approximately 0.01 Hz to 10 Hz. In addition, the system is capable of operating unattended for approximately seven months, and the only operator requirement is to change the data storage disk at the end of the seven months.

The MAI Generation System can generate spectral information in frequency bandwidths of order of 7.32 mHz (136 second period) and these individual frequency bands can be combined to cover larger frequency bands that may be of interest. The system can be set to record spectral information in several such frequency bands, and the number of these bands is limited solely by the storage capacity of the system. There are no restrictions on whether these bands have to be overlapping or non-overlapping, although the larger the desired number of bands the larger the amount of data recorded by the MAI Generation System and so more frequent operator visits would be required to install new data storage discs.

Figure 1: The large dots indicate the geographic locations where the East and West Coast MAI Generation Systems were operated.

The indices stored in the system can be retrieved at any time by communicating with the MAI Generation System via telephone line. This communication capability is an important aspect of the system, as it allows for the unattended operation of the system over several months. The system is capable of responding to a variety of user requests and inquiries concerning the data and other operational information of the system, and up-to-date information about the magnetic activity at the site can be obtained whenever desired.

The system cost was kept as low as possible to facilitate the ultimate deployment of a number of units. The approximate hardware cost for each of the systems was approximately $5000.

The first Magnetic Activity Index Generation System was successfully tested at Monterey, California (geographic: 36°35′N, 121°55′W; geomagnetic: 43°00′N, 58°33′W) for approximately six months from July 1986 to January 1987. A second system was then constructed and the two systems were operated at Corralitos, California (geographic: 36°59′N, 121°48′W; geomagnetic: 43°23′N, 58°31′W) and Grafton, New Hampshire (geographic: 43°34N, 71°57′W; geomagnetic: 54°35′N, 1°13′W). Figure 1 shows the geographic locations of the two MAI Generation Systems. These systems have successfully provided indices of magnetic activity on the West and East coasts of the U.S.

# 2 Overview of the MAI Generation System

Each MAI Generation System is a computer-based signal processing system in which the computer initiates all the data processing tasks and responds to user interactions either from the keyboard or across telephone lines.

Each system has two main sections that are connected to each other via a 500 ft cable. The first section consists of the computer and the signal receiving circuitry. These are normally housed in a shed or other shelter which is equipped with ac power and a telephone line. The second section of the MAI Generation System, located at the input end of the 500 ft cable, consists of the low noise amplifiers and magnetic field sensor. Separation of the two sections is needed to keep the sensors away from the electromagnetic signals generated by the equipment in the shed. Figure 2 shows the general arrangement of the components of the system, and the individual subsections are described in Section 4.

The sensors for the MAI Generation System are solenoidal coils of aluminum wire enclosing high-permeability steel cores. The variation of the magnetic field through the coil generates very small voltages at its terminals, which have amplitudes of the order of several hundred nano-volts. These voltages are amplified by low noise amplifiers with an overall voltage gain of approximately 118 dB (800,000 times). The amplified signals are then sent back to the shed by a set of differential line drivers. Differential line drivers are used to minimize external noise pick up.

The transmitted differential signals are received in the shed by a differential amplifier. The difference signal is then amplified if necessary, to achieve approximately a one volt amplitude level, and is then passed through a sharp anti-aliasing filter before it is sampled. The filtered signal is sampled at a rate of 30 samples per second by an 8 bit analog-to-digital converter. Finally, the digital stream of data is sent to the computer, which constantly processes the incoming data samples without any loss of data.

The relative response of the analog section of the MAI Generation System to a fixed amplitude sine wave magnetic signal is shown in Figure 3. The data were obtained during a calibration procedure using a known sinusoidal source of magnetic field and stepping through the frequency ranges of the system. At frequencies less than 0.1 Hz the response of the system was not practically observable due to the limits of the calibration circuitry, but it can be expected to follow the slope downward until about 0.01 Hz. The increase in the relative response of the system as a function of frequency is due to the increase in the induced voltage across a coil as the frequency of the incident magnetic field is increased. That is, if the magnetic field applied to the coil sensors is

$$B(t) = B_0 \sin(\omega t) \tag{1}$$

then the voltage induced across the coil terminals is

$$V(t) = \mu_r A_c N \frac{dB(t)}{dt} = \mu_r A_c N B_0 \omega \cos(\omega t) \tag{2}$$

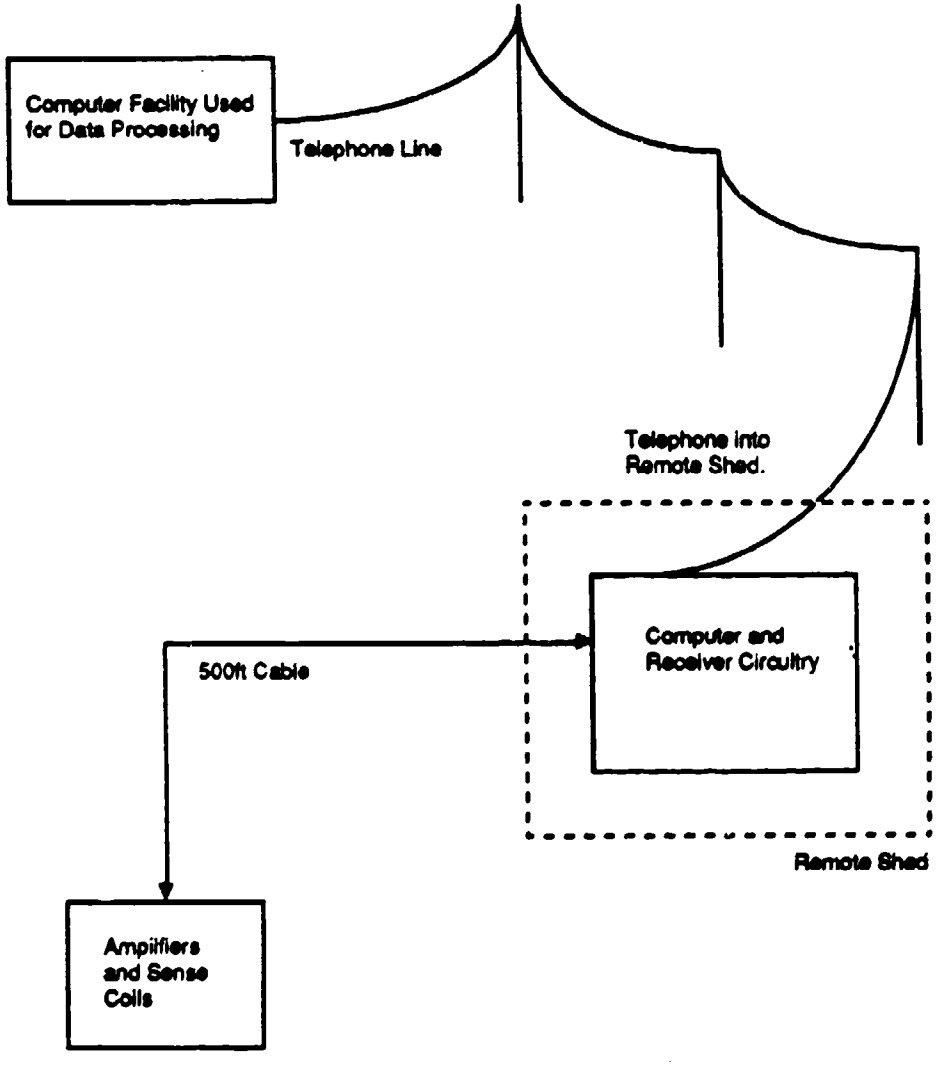


Figure 2: The MAI Generation System consists of two main sections which are separated by a 500 ft cable. The computer and receiving circuitry are housed in a shed and send dc power out to the amplifiers near the sense coils.

where $N$ is the number of wire turns of the coil, and $A_e$ is the *effective* cross sectional area of the coil. We can represent the effective area as

$$A_e = \frac{A - a}{\mu_r} + a \tag{3}$$

where $A$ is the cross sectional area of the coil, and $a$ is the cross sectional area of the core. The relative permeability of the core material is denoted by $\mu_r$, and it is in general a non-linear element that can depend both on the frequency of the applied magnetic field, and the level of that field. The core material can saturate at large signal levels, but such large signal levels are not expected from exposure to natural geomagnetic activity.

In the MAI Generation System the value of $\mu_r$ is approximately 10 to 20, depending on the core used, and it remains constant over the frequency range of the system. One can rewrite

$$V(t) = C\omega \sin(\omega t) \tag{4}$$

where $C$ is defined as

$$C = \mu_r A_e N B_0 \tag{5}$$

Thus, the induced voltage increases linearly as the frequency is increased, with the slope being approximately equal to 1 on a log-log plot.

The digitized stream of data is processed continuously by the computer. The data are collected in blocks of 4096 samples (136 seconds of data) and frequency analyzed. A fast Fourier transform (FFT) is performed on the data after multiplying the data by a 4096 point Hamming window. The power spectrum of the transformed data is then computed and the average power in various desired frequency bands is calculated. The averaging reduces the statistical variance of the power spectrum estimates. This process is constantly repeated and it generates a set of spectral estimates every 136 seconds. The statistical variance of the spectral estimates is further reduced by the method of averaging non overlapped modified periodograms [*Welch*, 1967]. The averaging is performed over half hour intervals, which include 13 or 14 spectral estimates (depending on the exact timing of the transform operations) and the results are stored every half hour. The above averaging technique has the unavoidable effect of reducing the time resolution of the estimates to half hourly.

The information stored in the MAI Generation System is the logarithm to the base two of the half hourly average of the average power spectrum in the various frequency bands. These numbers comprise our MA indices, and currently there are 12 such numbers generated every half hour, covering 12 frequency bands in the 0.01 Hz to 10 Hz range. Table 1 lists the 12 frequency bands, together with the FFT bins that are used in calculating each MA index. Notice that the MA3 through MA11 bands span the 0.01 Hz to 10.0 Hz frequency range without gaps and without overlapping, whereas the MA0, MA1 and MA2 bands cover frequency ranges that overlap each other as well as parts of the other nine ranges.

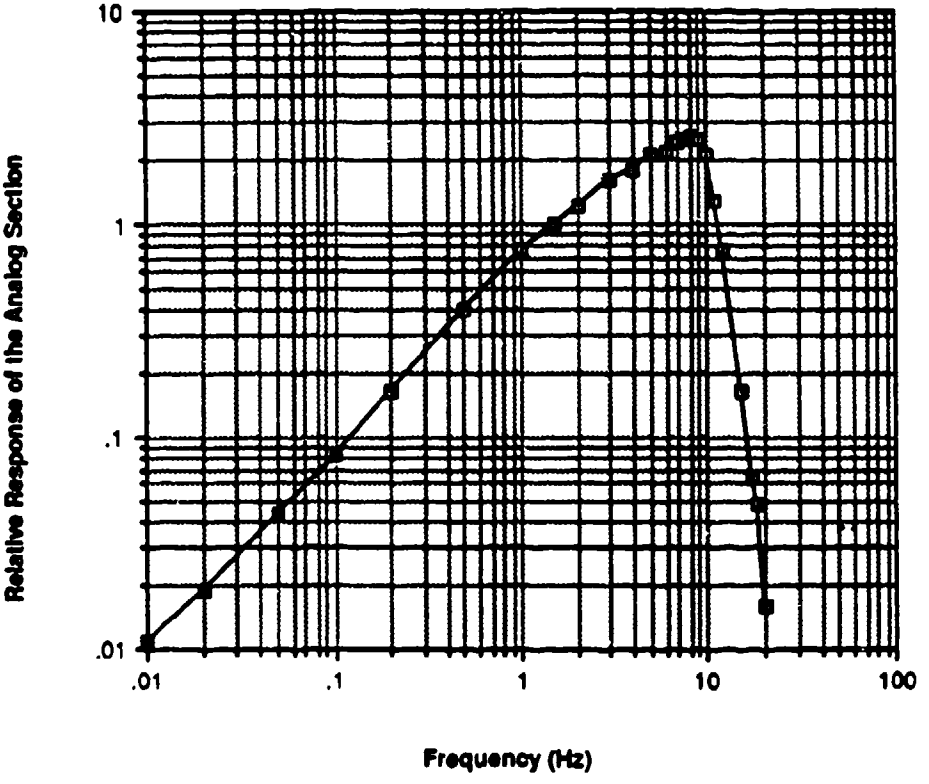


Figure 3: The relative response of the analog section of the MAI Generation System. In practice an incident magnetic field of 100 m$\gamma$ peak-to-peak sine wave will generate a signal level of 2.6 volts peak-to-peak at the maximum point of the plot. Measured values are shown by hollow boxes and interpolated ones are the solid boxes.

Table 1: The 12 MA indices are calculated from the average power in the following 12 frequency bands. Note that the MA0, MA1, and MA2 bands overlap others.

| MA Index | Frequency Band (Hz) | FFT Bins |
|---|---|---|
| MA0 | 0.04 - 0.20 | 5 - 27 |
| MA1 | 0.04 - 0.60 | 5 - 82 |
| MA2 | 0.20 - 2.00 | 27 - 273 |
| MA3* | 0.01 | 2 - 2 |
| MA4 | 0.02 - 0.04 | 3 - 6 |
| MA5 | 0.05 - 0.10 | 7 - 13 |
| MA6 | 0.10 - 0.20 | 14 - 27 |
| MA7 | 0.21 - 0.50 | 28 - 68 |
| MA8 | 0.51 - 1.00 | 69 - 136 |
| MA9 | 1.00 - 2.00 | 137 - 273 |
| MA10 | 2.01 - 5.00 | 274 - 682 |
| MA11 | 5.00 -10.00 | 683 - 1365 |

* Only one FFT bin included.

The MA0, MA1 and MA2 frequency bands were chosen specifically for their relevance to MAD operations. The nominal MAD frequency range is 0.04 to 2.0 Hz, which includes at least two and perhaps more independent classes of magnetic activity (depending on the geomagnetic latitude; at high latitudes there are more variations of magnetic pulsations). These classes of activity are discussed in Section 3. We have divided the nominal MAD frequency range into approximately three MA bands; MA0, MA1 and MA2. The MA1 band corresponds to a typical setting of the MAD equipment, and it includes the frequency ranges of the Pc 1, Pc 2, Pc 3, and Pi 1 geomagnetic pulsations. The study of the MA1 index, in particular, demonstrates the variation in magnitude of magnetic activity that can affect MAD equipment during normal operations. The MA0 and MA2 were chosen because they cover magnetic activity in the upper (MA2) and lower (MA0) halves of the nominal MAD band (0.04–2.0 Hz). Since MAD equipment has adjustable settings for lower and upper cutoff frequencies, these additional indices are used to study the distribution of the magnetic activity within and around the typical MAD equipment settings.

The MA3 index is derived from only one frequency bin of the frequency transform. Since the data are windowed prior to being transformed, this single frequency bin is affected by the adjacent bins. Thus, the values of MA3 should not be given a high significance. This single bin has been included in the MA indices to allow for studying larger frequency bands that start at the 0.01 Hz low frequency limit. In this report the MA3 index will be presented in the same manner as the remaining MA indices, even though we do not consider it to be as reliable as the others.

The MA indices can be related to absolute magnetic signal levels using the cali-

Table 2: Magnitude of the MA indices for 1 $\gamma$ peak-to-peak incident magnetic sine wave when the frequency of the sine wave is *exactly* in the center of the MA index bands. The third column is 2 to the power of (MA index), which is the average power per FFT bin. The last column is the average power per Hz of the incident magnetic field for the frequency band in study.

| MA Index | MA Index Magnitude | $2^{(MA\ Index)}$ | Average Power per Hz in Band $\gamma^2$/Hz |
|---|---|---|---|
| MA0 | 17.4 | $1.72 \times 10^5$ | 0.742 |
| MA1 | 18.5 | $3.59 \times 10^5$ | 0.219 |
| MA2 | 20.1 | $1.12 \times 10^6$ | 0.0691 |
| MA3 | 16.4 | $8.60 \times 10^4$ | 17.1 |
| MA4 | 16.4 | $8.91 \times 10^4$ | 4.27 |
| MA5 | 17.8 | $2.28 \times 10^5$ | 2.44 |
| MA6 | 18.8 | $4.61 \times 10^5$ | 1.22 |
| MA7 | 19.7 | $8.34 \times 10^5$ | 0.416 |
| MA8 | 21.0 | $2.07 \times 10^6$ | 0.251 |
| MA9 | 21.7 | $3.37 \times 10^6$ | 0.125 |
| MA10 | 21.5 | $3.05 \times 10^6$ | 0.0417 |
| MA11 | 21.9 | $3.87 \times 10^6$ | 0.0250 |

bration data in Figure 3. The second column of Table 2 shows the magnitude of MA indices when a 1 $\gamma$ peak-to-peak sine wave with a frequency *exactly* at the center of each MA band is incident on the sense coils (note that a 100 m$\gamma$ peak-to-peak sine wave is assumed for Figure 3). The additional assumption of the frequency of the incident wave being exactly at the center of the band is needed to allow the use of Figure 3. As the figure shows, the response of the system is not constant within an MA band. Note that when MA indices are calculated the input samples are scaled-up by 256 in order to reduce computational noise.

The third column of Table 2 is the average power per FFT bin before the logarithm calculation. The logarithm to the base two of the number in the third column is shown in column two. The last column of Table 2 is the average power per Hz of the incident 1 $\gamma$ peak-to-peak magnetic field for each of the MA frequency bands.

Data collected by the MAI Generation Systems at their remote sites can be accessed over the telephone, which is an important feature of the system. Up-to-date (up to latest half hour) power spectrum data can be obtained at any time by calling the desired MAI Generation System. Users can access any MAI Generation System whenever the telephone line to that site is free. In addition, the MAI Generation System has a number of HELP routines that allow new callers to find out about the capabilities of the system.

The MAI Generation System operation is highly automatic and needs no operator. As noted earlier, someone has to visit the remote site once every seven months to change the magnetic disk on which the half hourly MA indices are stored. All other system related operations can be performed remotely by communicating with the MAI Generation System via computer terminal, modem and telephone line.

In general, the MAI Generation System is capable of collecting and processing geomagnetic data while at the same time replying to requests received over the telephone line. The telephone callers must provide a user name, which functions as a password, and restricts access to the system data to authorized users. For the authorized users, the user name allows the system to assign two levels of priority to callers, thus allowing some delicate system related operations to be performed only by selected users. For example, the self calibration section of the MAI Generation System, which is usually turned off, may be activated by a caller who has sufficient priority. The calibration subsystem will then remain functioning until a request is received by the MAI Generation System for it to turn off the calibration subsystem. This calibration mechanism allows for a complete check of the MAI Generation System whenever desired, and for as long a period of time as is desired. In addition to this manual calibration circuitry, the MAI Generation System automatically activates the calibration circuitry at 11:30 pm UT every Sunday, and turns the calibration off just before midnight. Thus, for every week of data, one sample of calibrated data is provided automatically.

# 3 Naturally Occurring Magnetic Activity and Standard Indices

In this section we discuss several different types of naturally occurring geomagnetic activity with frequency bands overlapping those of the MAI Generation System. There exist various indices to describe the state of the geomagnetic activity either at a specific site, or for the whole Earth. Our MA indices also reflect the status of the magnetic activity, however, as will be shown, the MA indices have very different characteristics than the standard geomagnetic indices.

## 3.1 Types of Naturally Occurring Magnetic Activity

The 0.01 Hz to 10.0 Hz frequency range covered by the MA indices, includes a variety of naturally occurring magnetic activity. Some of the more common forms of this activity are known as magnetic pulsations, and these are listed in Table 3.

The Pc pulsations are usually referred to as regular pulsations because they are observed as regular sinusoidal waveforms of magnetic activity. They can be either continuous, or they can be observed as a train of sinusoidal pulses over a long time. The Pi pulsations, on the other hand, are usually referred to as irregular pulsations, and they are characterized by sudden occurrence of large pulses. The regular pulsations can

Table 3: Periods of the naturally occurring magnetic pulsations in the MA index bands.

| Label | Period (sec) |
|---|---|
| Pc 1 | 0.2 - 5 |
| Pc 2 | 5 - 10 |
| Pc 3 | 10 - 45 |
| Pc 4 | 45 - 150 |
| Pi 1 | 1 - 40 |

last from on the order of a few minutes up to several hours or more, with amplitudes of order of 1 m$\gamma$ to several $\gamma$. The irregular pulsations usually last up to tens of minutes, with amplitudes of up to several $\gamma$. The characteristics of the various classes of pulsation events are discussed in detail by *Jacobs* [1970].

The MA indices measure the power of the magnetic activity in the various MA frequency bands. The correspondence between the MA0 through MA11 bands, and the naturally occurring pulsation activity is shown in Table 4. It can be seen that some of the MA bands (either a single band or a combination) completely contain a certain class of naturally occurring magnetic activity. For example, Pc 2 is completely covered by the MA6 index, and Pc 3 is covered by the MA4 and MA5 indices. Note that MA11 is above the frequency range of the listed types of magnetic pulsations. However, some components of Pc 1 activity could extend into the MA11 band.

The MAI Generation System provides the researcher with a means for studying the statistical characteristics of geomagnetic activity in the Pc and Pi pulsation frequency bands, over a long period of time. The MA3 to MA11 indices are composed of non-overlapping frequency bands, and consequently the information in these bands can be combined to study a specific pulsation range. Not all of the pulsation frequency ranges can be matched exactly with the MA bands. However, due to the approximate nature of the frequency limits of the pulsation events, this limitation is not a significant one.

The time resolution of the MAI Generation System is half hourly, and so, half hourly up-to-date status information can be obtained concerning the magnetic activity in various pulsation frequency bands. Since most pulsation events have band limited characteristics, the MA indices can be used, at any time, to separate the background geomagnetic signals into active frequency bands and quiet frequency bands. This information can then be used to decide the frequency settings of MAD equipment.

## 3.2 Standard Indices for Naturally Occurring Magnetic Activity

There are a variety of different types of indices of geomagnetic activity currently in use. The more common indices are the *Kp* and *Ap* indices, where the letter *p* denotes 'planetary'. The planetary indices are generated by combining indices from thirteen

Table 4: Correspondence between MA indices and natural magnetic pulsations.

| MA Index | Frequency Band (Hz) | Natural Activity | | | | |
|---|---|---|---|---|---|---|
| | | Pc 1 | Pc 2 | Pc 3 | Pc 4 | Pi 1 |
| MA0 | 0.04 - 0.20 | | x | x | | x |
| MA1 | 0.04 - 0.60 | x | x | x | | x |
| MA2 | 0.20 - 2.00 | x | | | | x |
| MA3 | 0.01 | | | | x | |
| MA4 | 0.02 - 0.04 | | | x | | x |
| MA5 | 0.05 - 0.10 | | | x | | x |
| MA6 | 0.10 - 0.20 | | x | | | x |
| MA7 | 0.21 - 0.50 | x | | | | x |
| MA8 | 0.51 - 1.00 | x | | | | x |
| MA9 | 1.00 - 2.00 | x | | | | |
| MA10 | 2.01 - 5.00 | x | | | | |
| MA11 | 5.00 -10.00 | | | | | |

observatories located around the globe. For example, one of the observatories contributing to the $Kp$ indices is the Fredericksburg (USA) observatory, and the indices generated at that site are denoted by $K_{Fr}$. There is a direct correspondence between the $K$ and $A$ indices, with the $K$ indices being a quasi-logarithmic measure of the amplitude of the magnetic signals. These can be converted to the linear $A$ indices by the use of a simple look-up table.

At each station, the $K$ indices are generated by dividing every UT day into 8 three hour intervals, and then assigning a number between 0 and 9 to the observed range of magnetic activity during that time interval. The larger the observed activity at a station the larger the assigned $K$ index. The diurnal variations of the magnetic activity at each site are removed, as best as possible, and geographic location of the sites are taken into account when the 13 $K$ indices are combined to generate the $Kp$ indices. The computed $Kp$ indices consist of 28 levels, *i.e.*, 0o, 0+, 1-, 1o, 1+, ..., 9-, 9o. Detailed explanations of these indices are given by *Lincoln* [1967], *Jacobs* [1970] and *Rostoker* [1972], and a useful tutorial is presented by *Prochaska* [1980].

The most fundamental difference between the $K$ indices and the MA indices is that $K$ indices measure the maximum range of magnetic variations, over three hours, at a site, whereas, the MA indices measure the half hourly power of the magnetic activity in various frequency bands. Thus, the $K$ and $Kp$ indices can be affected by short term large amplitude pulsation events, whereas the MA indices are only affected by magnetic activity of longer duration. In addition, the $K$ and $Kp$ indices will be influenced by variations of the magnetic activity with periods of as large as 3 hours. Thus, they will not directly relate to the MA indices that are generated by our systems. In Section 6 and in Section 7 the $Kp$ indices and the MA indices will be compared to show the

differences between them.

# 4 Technical Description of the MAI Generation System

In this section technical details of the MAI Generation System are described. The system is a result of approximately 4 years of design and development, which included the construction of a simple prototype version during the early stages of the project [*Bernardi et al.*, 1985]. Attention was paid to making the system as small as practically possible, which resulted in the MAI Generation System taking up a small amount of space. At the computer end of the system about 8 square feet of bench space are needed for all the equipment, and at the sensor end about 4 square feet are needed for the low noise amplifiers, and 14 square feet for the coils.

The system power requirements are quite low. It uses approximately 100 W of power, most of which is due to the computer equipment. In addition, the system has been designed to operate in extreme temperature ranges that can happen in the East and West coasts. For example, the system at Grafton, New Hampshire has operated successfully at temperatures below $-20°$F.

The hardware building blocks of the MAI Generation System are shown in Figure 4. In the following we will describe each of these blocks.

## 4.1 Coils

The coils are made of 16 gauge aluminum wire wrapped around hollow plexiglass tubes. For portability, there are two identical coil sections, which are connected in series such that their induced voltages add. Each section has approximately 10,000 turns of wire and the wires are spooled from a diameter of 5.2 cm to 10.4 cm. The length of each section is approximately 80 cm. The core material used is a high-permeability steel rod. It has a length of 184 cm and a diameter of 3.7 cm.

The core extends through both of the coil sections. Thus, the overall coil dimensions are length of 184 cm, and a diameter of approximately 10.4 cm. The combined number of wire turns is approximately 20,000, and the total weight is about 40 kg.

The presence of the core material introduces a frequency dependence in both the series resistance and the series reactance of the coil equivalent circuit. These values were measured and recorded as a function of frequency. Both the reactance and resistance were found to increase as a function of frequency in such a manner that the $Q(=\omega L/R)$ of the equivalent circuit remained constant around 1 as the frequency was varied. This result is in agreement with previous studies of the properties of coils with cores [*Grossner*, 1983].

At the measurement sites the coils are placed horizontally in the magnetic East-West direction, with a wooden wind cover to avoid any wind-induced mechanical vibration

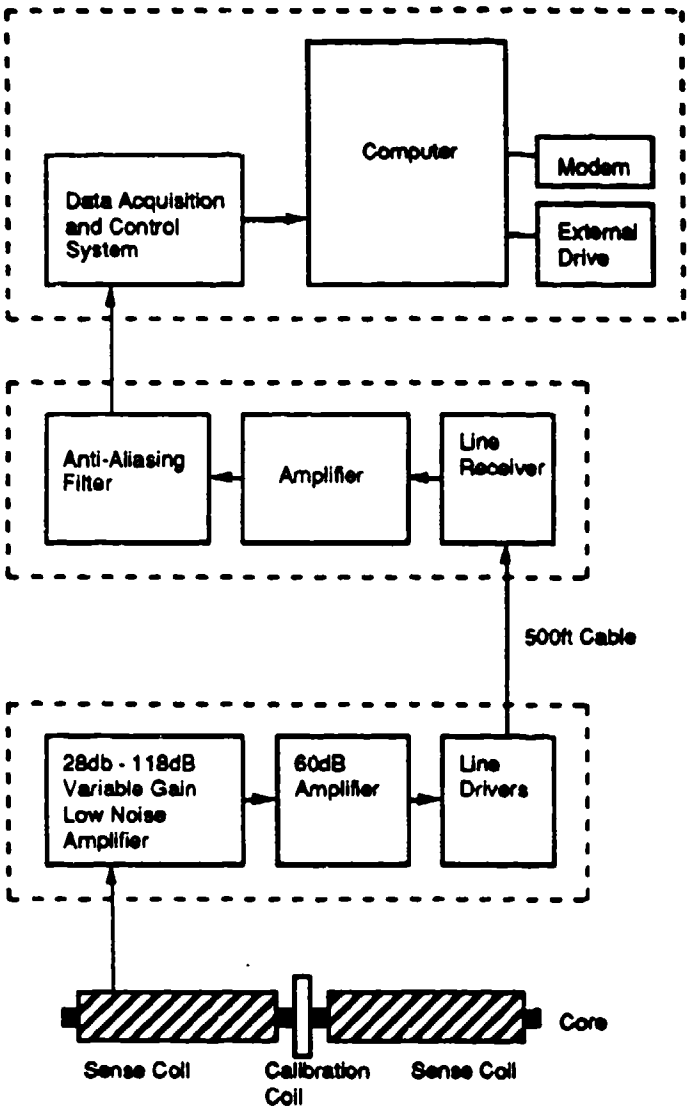


Figure 4: The functional blocks of the MAI Generation System and the interconnections between them.

of the coils.

## 4.2 Amplifiers

Almost all of the amplification of the voltages on the coil terminals is performed close to the coils by low noise amplifiers. The amplification takes place in two stages. The first stage is a Model 42.21 solid-state amplifier manufactured by Teledyne Geotech of Garland, Texas. It has a variable gain from 28 dB to 112 dB in steps of 6 dB. The amplifier has a band pass response with the lower 3 dB point at 0.005 Hz and the upper 3 dB point at 12.5 Hz, with second order rolloffs at each side of the band pass. The amplifier has an input impedance of about 4 k$\Omega$, and it is a differential amplifier. The output impedance of the amplifier is less than 10$\Omega$, and the noise level of the amplifier is 0.64 $\mu$V peak-to-peak for the 0.005–12.5 Hz passband at a gain setting of 58 dB. This unit is normally operated at a gain of 58 dB.

A second solid-state amplifier follows immediately after the one described above. It was designed by Dr. A. Phillips for use by the U.S. Naval Postgraduate School at Monterey, California, and it has a fixed gain of 60 dB, again with a band pass response. The lower 3 dB point is at 0.017 Hz and the upper one is at 20.0 Hz. The low end has a first order rolloff (6 dB/octave) and the upper end has the rolloff characteristic of a 3rd order (18 dB/octave) 3 dB ripple low pass Chebyshev filter.

## 4.3 Line Drivers

The line drivers are used to send the amplified signal across two differential lines that link the amplifiers near the coils with those at the computer through approximately 500 ft of cable. The use of differential line drivers greatly reduces the noise added to the signal over the 500 ft of cable.

## 4.4 Line Receivers

The line receivers combine the differential signals received from the line drivers to produce one single ended signal. Thus, any noise signal that is coupled into both wires is subtracted from the signal at this stage.

## 4.5 Receiver Amplifier

The receiver amplifier is used to amplify the signal from the line receivers in order to achieve desired voltage levels. Normally, this amplifier is set at a gain of 0 dB, since it is preferable to amplify the signal fully at the stages closest to the coils, in order to reduce the effects of noise pick up.

## 4.6 Anti-Aliasing Filter

The amplified signal is sampled at a rate of 30 samples per second. The anti-aliasing filter is built to account for that sampling rate. The filter is a 6th order Butterworth low pass filter with 3 dB cutoff at 10.0 Hz. The filtered signal is then biased at +2.5 Volts and sent to the analog to digital converter.

## 4.7 Analog to Digital Converter

The analog-to-digital converter is an $8\pm\frac{1}{2}$bit converter. It is part of a microprocessor-controlled data acquisition and control system, Model Number 8232, manufactured by Starbuck Data Company of Wellesley, Massachusetts. The system receives and transmits commands on an RS-232 communication line to the computer. The analog signals are allowed to vary in the range of 0 to 5 Volts, therefore requiring the +2.5 volt biasing of the signals before being digitized. The effect of the biasing is later removed during the computer processing of the digitized samples.

## 4.8 Computer

The computer used in the MAI Generation System is a Macintosh Plus personal computer manufactured by Apple Computer of Cupertino, California. The computer is connected to an external disk drive with an 800K byte storage capacity. All the MA indices are stored on the $3\frac{1}{2}$inch disk in the external drive. A similar internal drive holds the software and data files needed for the operation of the MAI Generation System. In addition, the computer is connected to the telephone lines through a 1200 baud modem.

## 4.9 Calibration System

The calibration process can be initiated either during a telephone connection, or directly from the keyboard of the computer. This allows a user to perform a calibration for a long period of time. This feature is needed when, for example, calibration data are desired for a whole day to check for any diurnal temperature effects on the analog hardware. The MAI Generation System also automatically initiates a calibration for half an hour once every week. The calibration circuitry used in the MAI Generation System induces a known signal into the coils through magnetic coupling. This is performed by sending a pulsed current through a calibration coil which consists of a single turn of wire positioned in the middle of the two halves of the sense coils. The computer generates the calibration signal by sending instructions to the data acquisition and control system to close and open a transistor switch at a rate of 1.5 Hz. This switch causes a known current to flow from the power supplies present in the line receiver, across 500 ft of cable, through the single turn calibration coil, and back across the 500

ft cable. The magnetic signals generated by the calibration coil are picked up by the sense coils, and checked for proper operation of the MAI Generation System.

## 4.10 MAI Generation System Software Features

The software used in the computer was specifically written for this project. Various software features of the system which have not been discussed above will now be presented.

The comparatively remote locations in which an MAI Generation System needs to be operated are likely to be subject to occasional ac power failures. The MAI Generation System is therefore programmed in such a way that it can start up properly after any power failure, at which time it instructs all the connected hardware units to reinitialize and begin their operations. When the MAI Generation System software begins operation it initializes the data acquisition system to sample the analog signal at 30.0 samples per second continuously, and the modem to answer the phone on the first ring. The program then proceeds with various internal parameter initializations. Typical parameters are the sine and cosine arrays used for the Fourier transforms; the variables used for error detection; the display related parameters; and the serial driver parameters. Upon completion of all initializations, which takes a couple of minutes, the MAI Generation System begins its data processing.

In order to keep timing of data records intact, the computer writes a date/time entry in the MA indices file before the first valid indices are written The format of this file is as follows. Timing marks are inserted into the data stream at 00:00 hours every UT day. The 00:00 UT mark is followed by a line of MA indices which are written immediately following the writing of the 00:00 mark, and thus they measure the magnetic activity occurring from 23:30 UT to 00:00 UT. The next line of MA indices is written at 00:30 UT, and these MA indices measure the magnetic activity occurring during the 00:00 to 00:30 UT interval, and so on. There are no timing marks written for these lines, since their time can be easily calculated from the 00:00 marks of each UT day, thus reducing the storage requirements of the MA indices file. As can be seen, during normal operation there are 48 lines of MA indices between the 00:00 date marks.

Additional status information is also stored in the MA indices file. The beginning and end of any calibration of the system is automatically stored in the file, so that the exact timing and duration of the calibration can later be verified. Similarly, timing information is stored in the data stream every time the system recovers from a power failure, thus allowing the user to find out the length of time power was lost to the system.

The MAI Generation System computer constantly checks for various error conditions that may occur during its operation. An example of an error condition is the presence of saturated signal levels at the analog-to-digital converter. If this form of an error occurs, either the dynamic limits of the system have been surpassed or an

analog component has failed, and consequently the MA indices are not reliable over that period of time. There are several such error conditions that the computer checks for and, if any occur, the exact time of the errors and their identification is written onto a separate errors file. From that point on, telephone callers are notified of the error condition, thus warning them that the MA indices are probably no longer valid and that corrective actions need to be taken.

Although the MAI Generation System normally operates completely unattended, the system can have some of its functions initiated through the keyboard, which is useful for diagnostic purposes. Power spectra can be seen in a plotting window on the screen, which is updated once every 136 seconds. In addition, in a text window, one can examine the actual data samples received from the data acquisition system or observe the latest MA indices.

Complete file recordings of the 4096 samples of data, together with the real and imaginary components of the FFT and the power spectrum of those data, can also be initiated through the keyboard. This allows for checking of the routines which process the digitized data.

# 5 Initial Measurements at San Francisco Bay Area

As was described in the introduction, there are a variety of sources of low frequency magnetic noise in city environments, which necessitates the operation of MAI Generation Systems at remote sites. A good example of a strong source of urban noise is the subway system in the San Francisco Bay area. Some years ago our research group drew attention to the large-amplitude ULF electromagnetic fields being produced by the new dc-powered Bay Area Rapid Transit (BART) system that had been constructed in the San Francisco Bay Area [*Fraser-Smith and Coates*, 1978; *Ho et al.*, 1979; *Samadani et al.*, 1981]. In that work it was shown that the BART system generates magnetic field fluctuations, measured at Stanford University, of up to two orders of magnitude larger than the natural background geomagnetic signals. These measurements were made in a frequency band centered at 0.2 Hz with a bandwidth of 0.1 Hz. For measurements made closer to BART, the signal was observable in the larger 0.001 Hz to 10 Hz frequency range.

When development of the MAI Generation System was completed, it was decided to test the system performance at a Stanford University site. It was expected that the BART-generated magnetic fields would be clearly evident in the measurements made by the system. The MAI Generation System was set up locally and the system was left running from March to June, 1986. The data collected during that time interval predominantly measured BART-generated magnetic noise.

Figure 5 is a plot of the magnetic indices generated by the MAI Generation System during the week beginning Sunday April 20, 1986. The daily variation of the strength of the activity follows a repetitive pattern from Monday through Friday. The magnetic

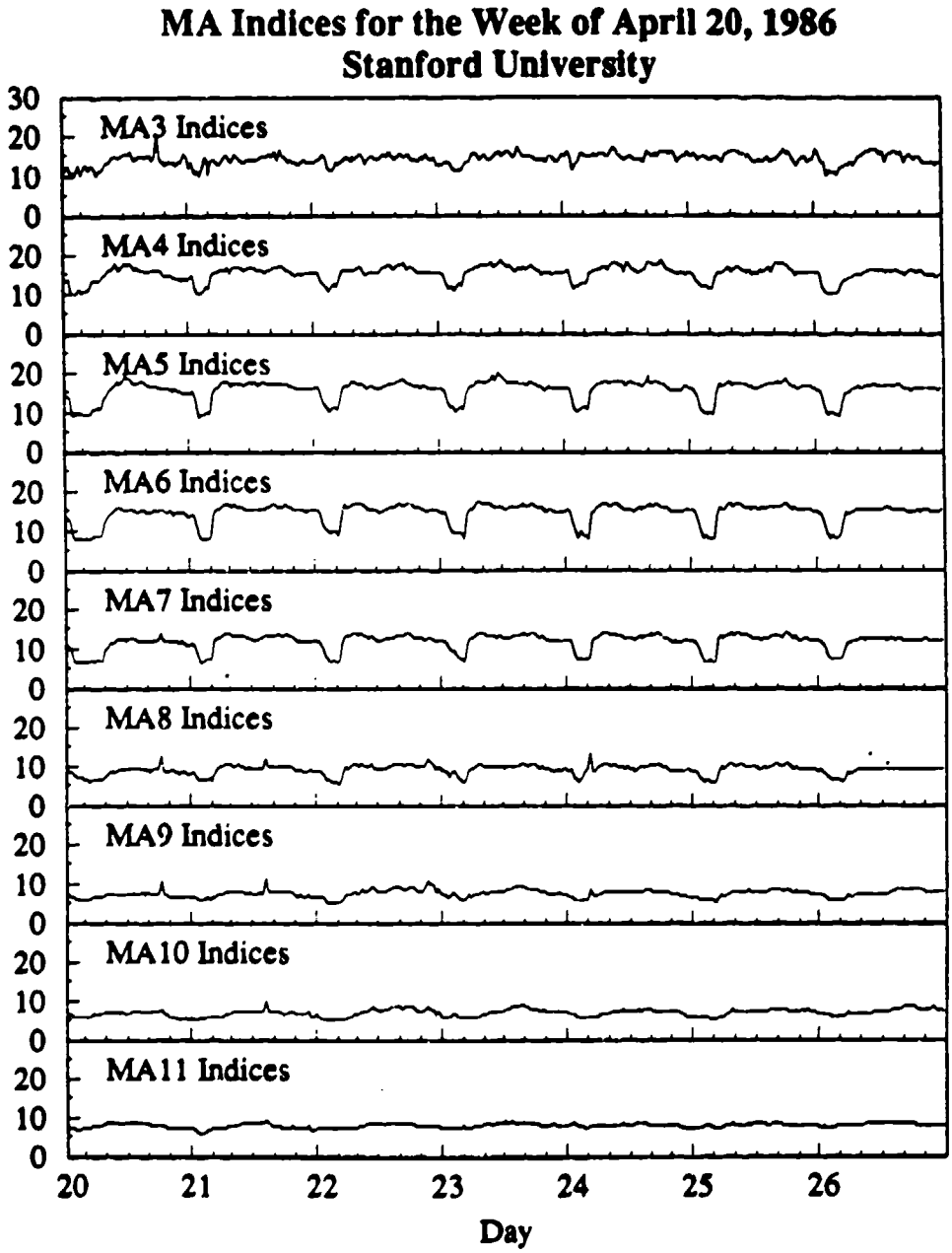


Figure 5: MA indices generated at Stanford University for the week of April 20, 1986. Note that the BART activity is concentrated in the 0.10 Hz to 0.20 Hz band, for which the corresponding index is MA6.

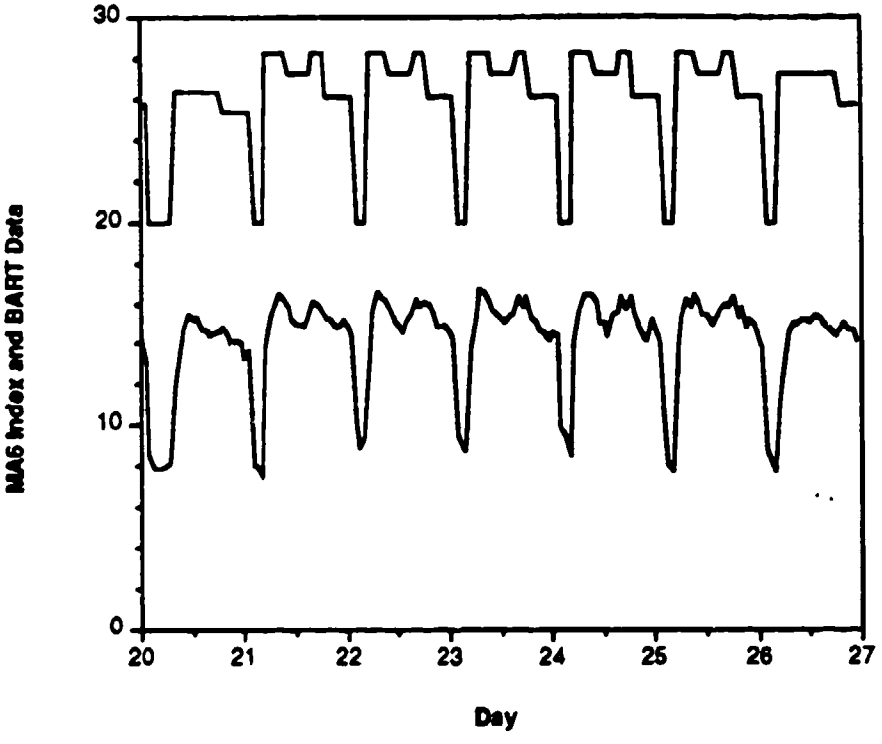


Figure 6: Comparison of magnetic activity measured at Stanford University with the number of BART cars. The lower plot shows the MA6 index generated at Stanford University for the week of April 20, 1986, and the upper plot is 20 plus the logarithm of the average number of train cars operated by the BART system. Notice the strong correlation between the index and the average number of train cars.

variations for Saturday and Sunday are slightly different, as might be expected. The figure shows that the BART activity is concentrated mostly in the 0.10 Hz to 0.20 Hz frequency band, corresponding to the MA6 index.

We contacted BART public affairs [*Patubo,* 1986] to find out the average number of train cars that are operating on the tracks as a function of the time of day. Note that the BART system, as any other train system, adds and removes train cars from a train depending on the demand, so that the load of the system is related to the total number of cars in use, as opposed to the number of trains.

The magnetic field fluctuations generated by BART appear to have amplitudes that are proportional to the change in the dc current used by the trains as they acccelerate and decelerate. We assume that during steady state, when the trains are either in full motion or completely stopped, only negligible magnetic field fluctuations are produced. Thus, the power spectrum of the magnetic field, which is proportional to the square of the field, is proportional to the square of the currents in the BART system, which itself is proportional to the average number of train cars in operation. We thus need to plot the logarithm of the average number of cars running on the BART tracks as a function of time of day and compare it with the logarithm of the average power in each of the frequency bands, *i.e.*, MA indices.

Figure 6 is a plot of the MA6 index and the logarithm of the average number of train cars as a function of time of day. The value of 20 has been arbitrarily added to the BART logarithms in order to display the BART 'indices' above the MA6 values. In addition, at times when the BART system is not functioning, in which case the logarithm of the average number of train cars would be $-\infty$, the value has been set to 20. Figure 6 clearly shows the strong effect of BART activity on the low frequency magnetic signals observed at Stanford.

The BART-generated magnetic activity has a regular Monday through Friday pattern, corresponding to the morning rush hour, reduced service during the day, an afternoon rush hour followed by a further reduced service for the evening, and finally the end of service. The weekend activity takes a different form. On Saturdays, BART begins its operations the same time as Mondays through Fridays, but only provides two levels of service for the day. On Sundays BART system starts its service later than the usual time of 4:30 am local time, and again provides only two levels of service for the day. All of these features can be seen in the MA6 indices of Figure 6.

# 6 Initial Measurements on the West Coast

Following the successful test of the first MAI Generation System at Stanford, the system was moved to a location far enough away from the BART system to avoid contamination of the MA indices by BART generated signals, and thus to allow study of the MA indices produced by naturally occurring magnetic activity. The new location was in Monterey California, in a remote part of the Naval Postgraduate School grounds near the La Mesa Village student housing section.

## 6.1 West Coast MA Indices

The MAI Generation System operated successfully from mid July 1986 until mid January 1987 at its Monterey location. Figure 7 shows variations of nine of the MA indices (MA3 to MA11) covering the frequency response of the system in non-overlapping bands from 0.01 to 10.0 Hz, for the month of September, 1986. It can be seen that there tends to be more activity in the low frequency MA indices than the high frequency ones, although there is a rather regular periodicity present in the high frequency MA indices. There also seems to be a null in signal activity in the middle frequency bands, as measured by the MA6 index, for example. Note that since MA indices are logarithmic, the increase in the MA indices observed on the 12th of the month, approximately by a value of eight, corresponds to an increase of the power of the signals by a factor of 256.

The MA indices can be compared with the standard $Kp$ indices. The $Kp$ indices are planetary indices, and are themselves an average of magnetic activity observed in 13 recording stations around the globe (see Section 3). Since the $Kp$ indices are three hourly range indices and MA indices are half hourly power spectrum indices, one would expect that during strong magnetic activity of long duration both the $Kp$ and MA indices would tend to be large. On the other hand, large $Kp$ indices would not necessarily indicate large MA indices, and vice versa, since, for example, a short lasting magnetic disturbance may register a large $Kp$ value, but would not tend to be significant when averaged over a half hour for the MA indices.

Figure 8 shows a plot of the $Kp$ indices for the month of September 1986. The large $Kp$ indices for the 12th and 23rd of the month match the large activity indicated by the MA indices plots. The activity of the 12th is present in most of the MA indices, whereas the activity of the 23rd is present only in the lower MA indices. However, the frequency bands in which the magnetic activity is large are not necessarily in a connected set; for example, the activity of the 14th is present in both the low and high MA frequency bands but is missing in the middle MA indices. Those data therefore give added information about the frequency content of the magnetic activity present in the Monterey, California, area. An additional noticeable fact is that the MA indices have a diurnal variation when a magnetic storm is in progress, whereas in the $Kp$ indices all the diurnal variations have been removed. An example of the diurnal variation is seen in the MA5 index for the few days following the 12th and the 23rd.

There is a striking periodicity present in the MA11 and MA12 indices. The daily variation of the magnetic activity is at a minimum at the MA12 index at about 12:00 UT, which accounts for magnetic activity from 11:30 UT to 12:00 UT. The signal then increases to a peak at about 16:00 UT and stays at a flat level until about 03:00 UT when it begins to drop. Initially, these periodic variations were thought to be those of the naturally occurring magnetic activity. However, after the system was moved to another site, approximately 30 miles away, most of the regular periodicities present in the MA11 and MA12 indices disappeared. It is now believed that the signals observed in the high MA indices were largely due to the nearby housing environment (perhaps relating to

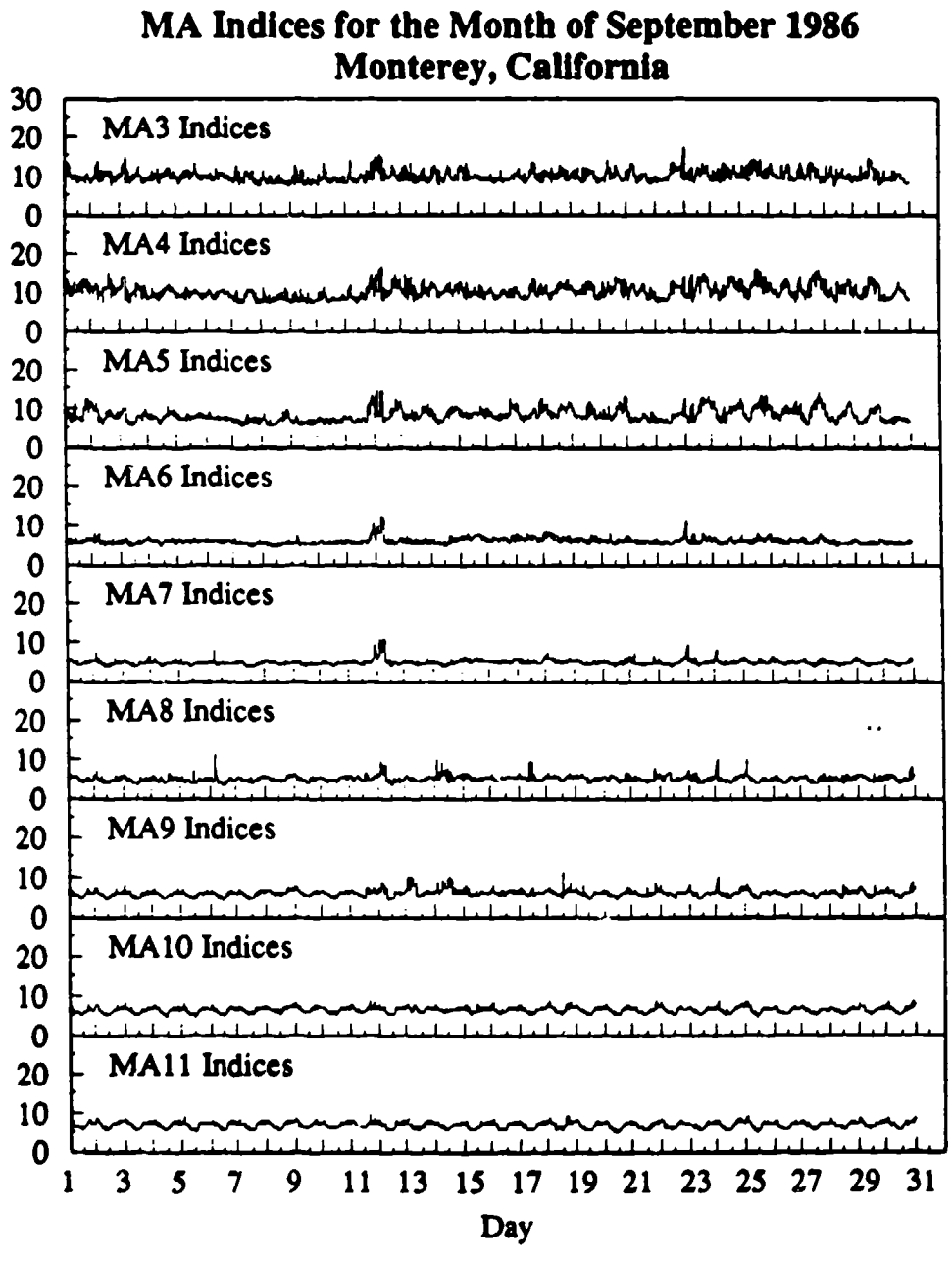


Figure 7: Plots of nine MA indices generated at Monterey, California for the month of September 1986.

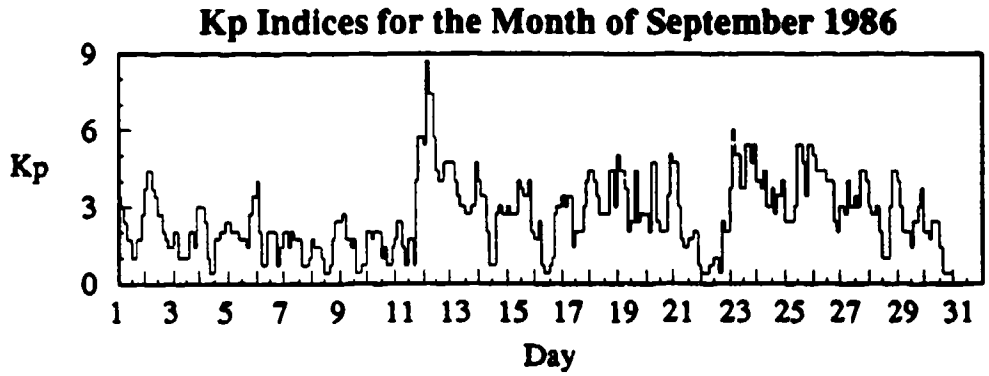


Figure 8: $Kp$ indices for the month of September 1986.

electric current increases and decreases) and that the strong 24-hour periodicities in the MA11 and MA12 indices are due to man-made noise.

## 6.2 Autocorrelations of West Coast MA Indices

An important item of information that can be obtained from the MA indices is the autocorrelation function of each of the indices. The autocorrelation function indicates the extent of linear dependence between an MA index at a certain point in time and the same MA index at a later time. Cross correlations between various MA indices at the same site are not considered in this report.

An estimate of the autocorrelation at lag $k$, $\hat{R}_M(k)$ can be derived as follows. Note that we will use a $\hat{}$ to represent an estimated quantity. We first define the estimate of the autocovariance function at lag $k$, $\hat{K}_M(k)$, as

$$\hat{K}_M(k) = \frac{1}{N} \sum_{i=0}^{(N-1)-k} (M_M(i+k) - \overline{M_M})(M_M(i) - \overline{M_M}) \tag{6}$$

where $N$ is the number of data points, $M_M$ can be one of MA0,...,MA11 indices at Monterey, and $\overline{M_M}$ is the mean of the Monterey data. Note that the correlation lag $k$ can vary from 0 up to and including lag $N-1$.

The autocorrelation is then the normalized autocovariance and is given by

$$\hat{R}_M(k) = \frac{\hat{K}_M(k)}{\hat{K}_M(0)} \tag{7}$$

Nine autocorrelation plots are shown in Figure 9 for lags of up to one week. These autocorrelations were calculated using Monterey data from the month of September, 1986. There is significant daily correlation between most of the MA indices. The correlation is strongest for the magnetic activity repeating every 24 hours, and is weakest

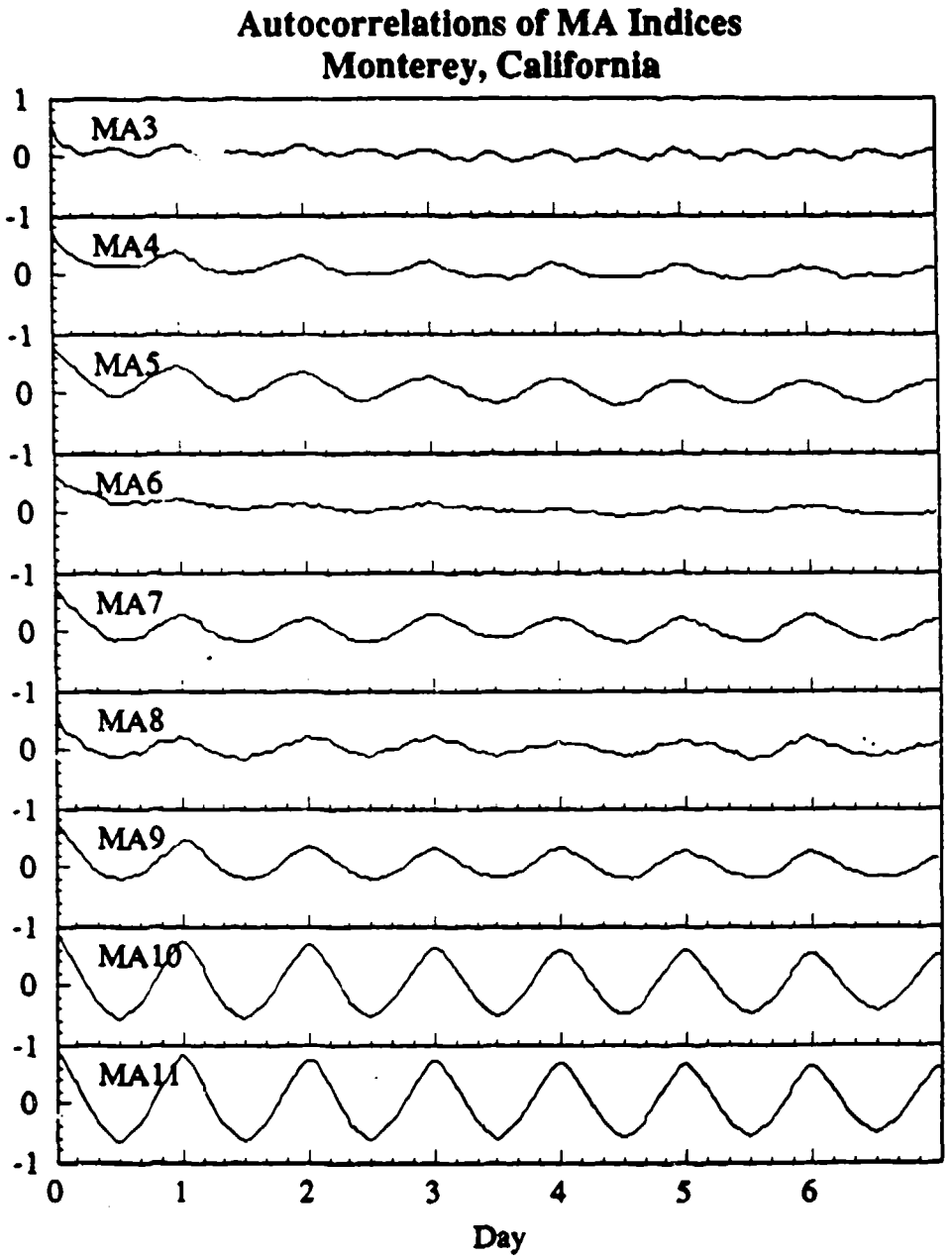


Figure 9: Nine plots showing the autocorrelations of the MA indices MA3 through MA11 generated at Monterey.

for activity that lags by 12 hours (repeating every 24 hours). The strong correlation is absent in the MA6 and MA8 indices, however. One can also see the large correlation of the high MA indices, thus indicating the strong non-random nature of those indices.

# 7 Simultaneous Measurements on the East and West Coasts

Operation of the first MAI Generation System was terminated at Monterey in February 1987 and the system was returned to Stanford University for certain modifications and improvements. Concurrently, a second system was built similar to the improved MAI Generation System and was again tested at Stanford University. The two improved MAI Generation Systems were then relocated near the Pacific and Atlantic coasts of the United States (see Figure 1 and Section 1).

The second system was taken to a low-noise site near Grafton, New Hampshire, where it was installed and set in operation during September 1987, and the first system was taken to another low-noise site near Corralitos, California, where it began operation in October 1987.

## 7.1 East and West Coast MA Indices

Figure 10 shows the Corralitos MA indices for the week beginning November 9, 1987, during which unusually large activity was present in the low frequency bands. One can see a well defined diurnal variation in the MA5 index particularly when the magnetic activity reaches a high level towards the middle of the week. There is very little magnetic activity present in the higher frequency bands, indicating a strong band-limited nature for the signals that were observed during that week. It is also noticeable that the MA10 and MA11 indices do not have the diurnal variations that were observed in Monterey.

Figure 11 shows the MA indices again for the week of November 9, 1987, generated at Grafton, New Hampshire. The magnetic activity at Grafton has a larger overall magnitude than that of Corralitos, due to the higher magnetic latitude of the Grafton site [*e.g., Jacobs,* 1970]. Large magnetic activity is present in most of the MA indices of Grafton, although the largest activity occurs in the MA5 index, as was observed in the Corralitos data.

Figure 12 shows a comparisons of the MA indices generated at Corralitos for the week of November 9, 1987, with the $Kp$ indices for the same time period. Since most of the observed magnetic activity tends to be present in the lower MA indices, MA3–MA6, only the lower MA indices of Figure 10 have been plotted in Figure 12. One can immediately see that the $Kp$ indices lack the diurnal variation of magnetic activity observed at Corralitos. In addition, large values of the $Kp$ indices do not seem to correspond to any similar features in the MA indices. The MA and $Kp$ indices measure

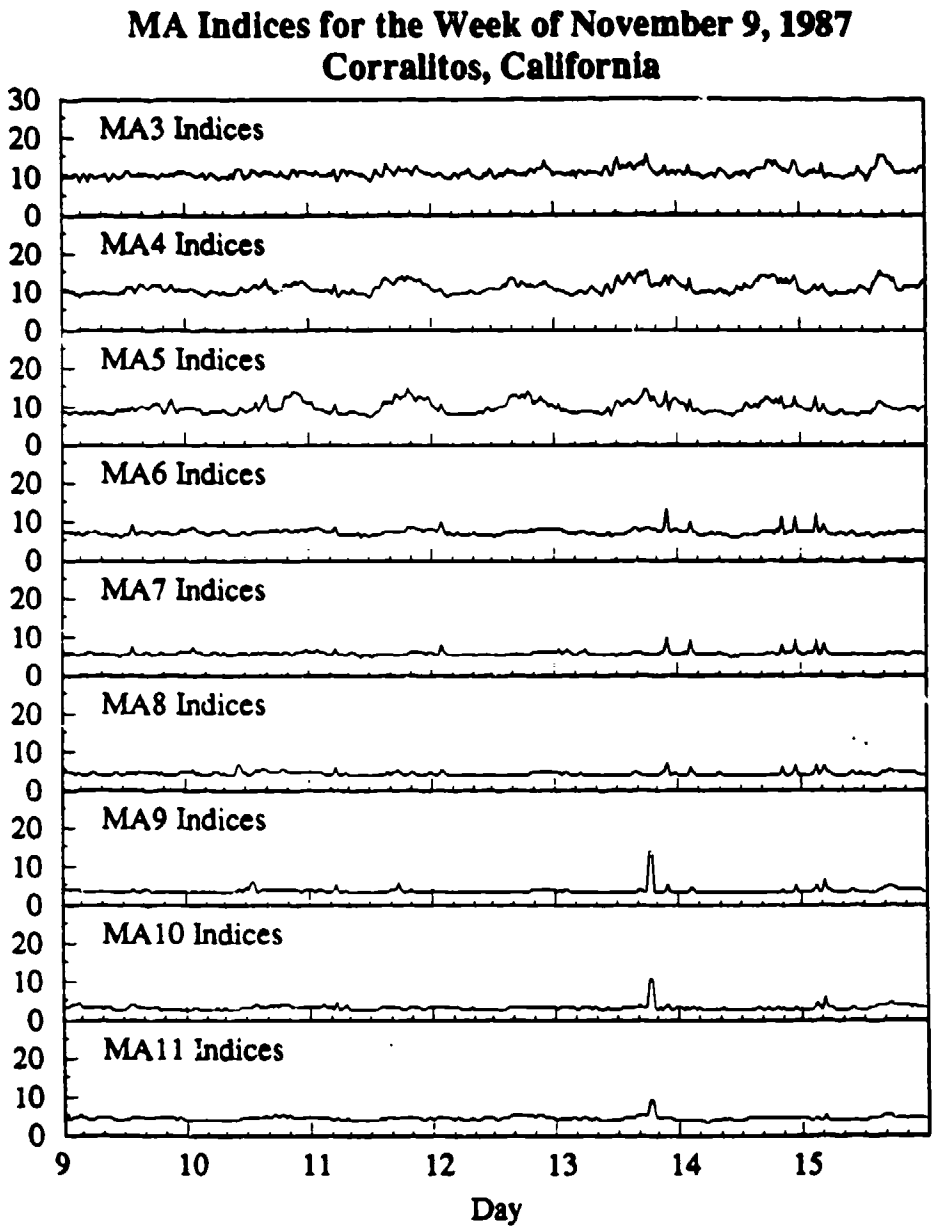


Figure 10: MA indices generated at Corralitos, California, for the week of November 9, 1987. The spike in the MA9, MA10 and MA11 indices on the 13th is due to a calibration test of the system.

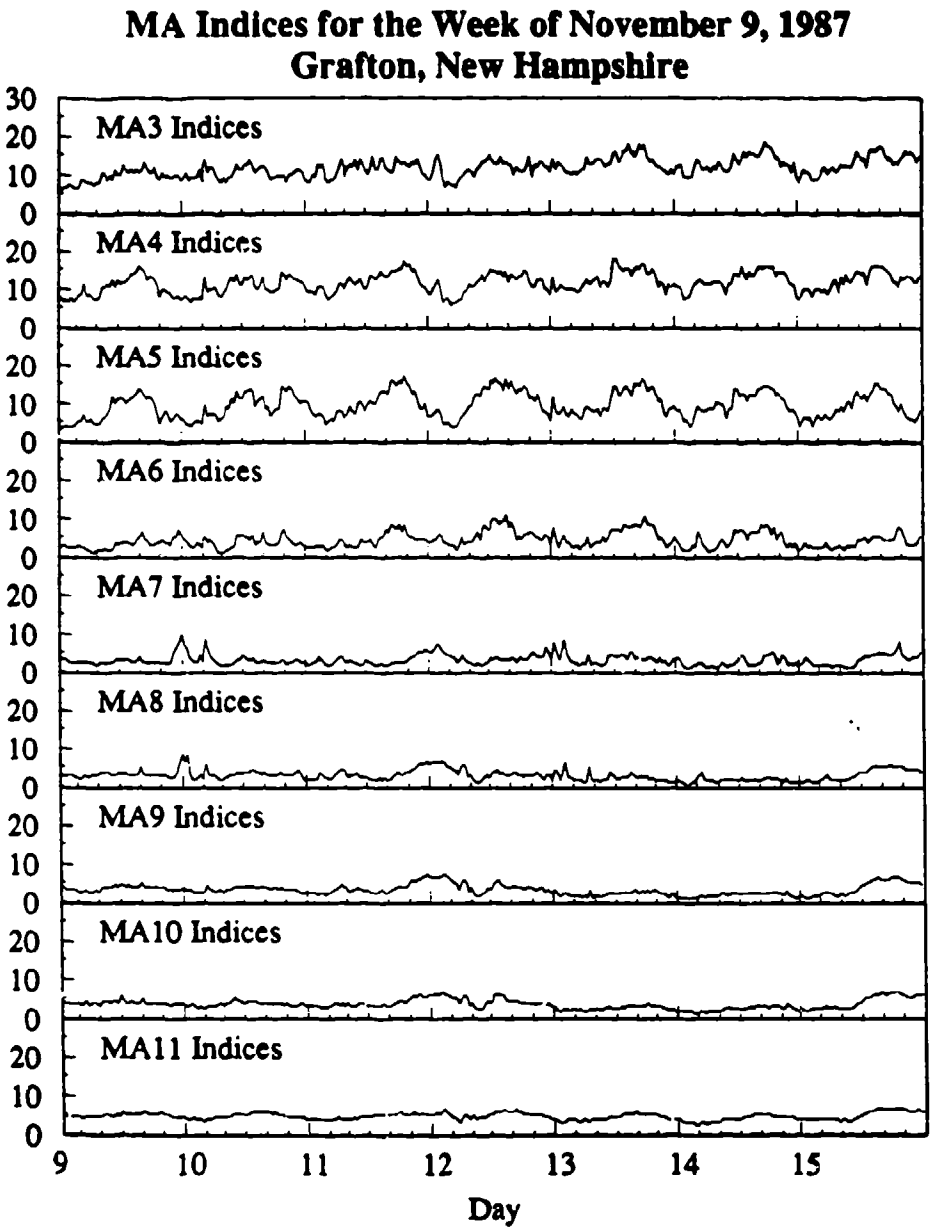


Figure 11: MA indices generated at Grafton, New Hampshire, for the week of November 9, 1987.

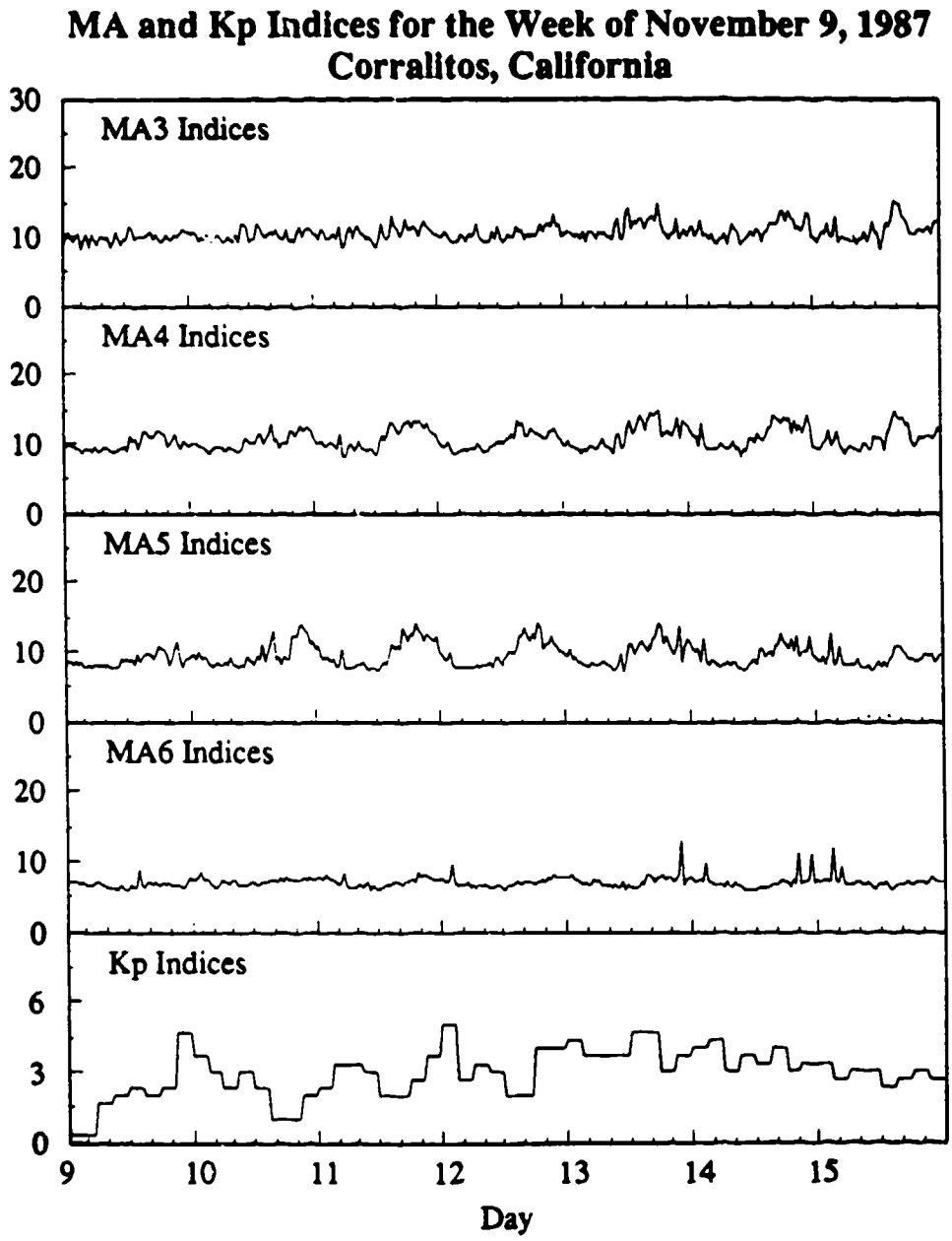


Figure 12: MA3, MA4, MA5 and MA6 indices generated at Corralitos, California, for the week of November 9, 1987, and the corresponding $Kp$ indices.

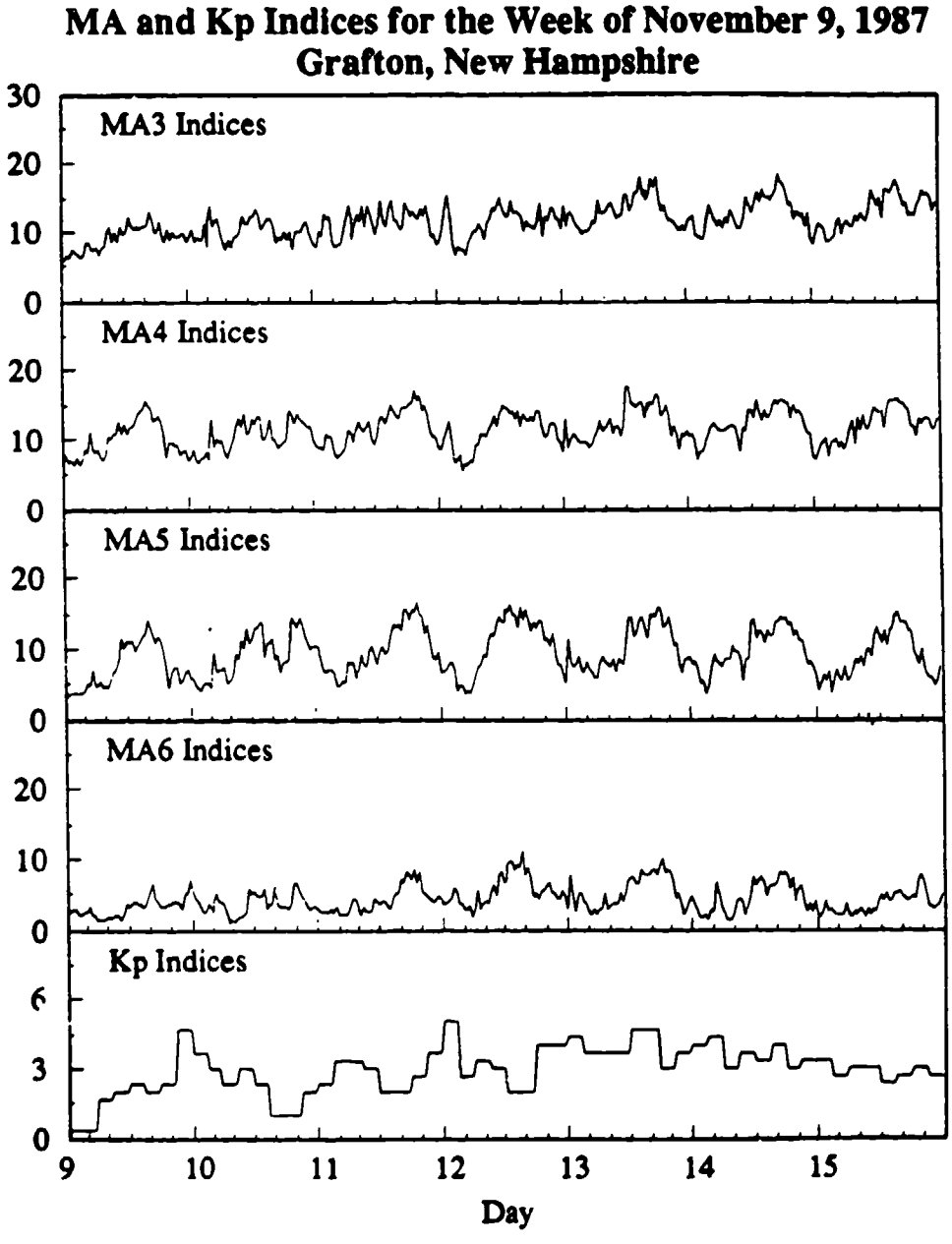


Figure 13: MA3, MA4, MA5 and MA6 indices generated at Grafton, New Hampshire, for the week of November 9, 1987, and the corresponding $Kp$ indices.

Table 5: Correlation coefficients between MA and $Kp$ indices for the Grafton and Corralitos data are shown. One week of MA indices were used (November 9, 1987) for calculating the correlation values.

| MA Index | Correlation Coefficients between MA and $Kp$ Indices (Grafton) | Correlation Coefficients between MA and $Kp$ Indices (Corralitos) |
|---|---|---|
| MA3 | 0.339 | 0.251 |
| MA4 | 0.107 | 0.126 |
| MA5 | 0.031 | 0.087 |
| MA6 | 0.185 | 0.109 |
| MA7 | 0.295 | 0.088 |
| MA8 | -0.018 | -0.140 |
| MA9 | -0.157 | -0.085 |
| MA10 | -0.247 | -0.133 |
| MA11 | -0.260 | -0.099 |

different features of the magnetic activity and they may correspond, for example, during periods of large magnetic storms when the range of magnetic activity and the average power of the activity can both be expected to be large.

In Figure 13 we have repeated the above comparison, but using the data from Grafton. Again, the diurnal variation of the magnetic activity shown in the MA indices is absent in the $Kp$ data. This figure shows an example of a correspondence between the MA and $Kp$ indices. The MA indices, particularly MA3 and MA4 show a short duration peak occurring just after 00:00 UT of the 12th. At the same time, the $Kp$ indices show a sudden increase of magnetic activity. We note, in addition, that the peak of the MA indices is concentrated mostly in the MA3 and MA4 indices, and is rather small in the MA6 indices of the 12th. Thus, the MA indices can give indications of the frequency distributions of the magnetic activity at any time.

The correlation coefficients between the MA indices and the $Kp$ indices, at Grafton and Corralitos, are shown in Table 5. The table was calculated by using the MA and $Kp$ indices for the week of November 9, 1987. One can see there is very small correlation between the MA indices and the $Kp$ indices, at both of the sites. This confirms the fact that the two indices measure different aspects of the naturally occurring magnetic activity.

## 7.2 Autocorrelations of the East and West Coast MA Indices

Autocorrelations for the East and West Coast MA indices are shown in Figure 15 and Figure 14 for lags up to a week. These are calculated using the equations presented in

Section 6, which can now be rewritten as

$$\hat{R}_G(k) = \frac{\hat{K}_G(k)}{\hat{K}_G(0)} \tag{8}$$

and

$$\hat{R}_C(k) = \frac{\hat{K}_C(k)}{\hat{K}_C(0)} \tag{9}$$

where the subscripts $G$ and $C$ represent Grafton and Corralitos.

The autocorrelations were calculated using data from the month of January, 1988, at each location. A striking point to note is the lack of a strong daily correlation in the MA6, MA7, MA8, MA9 and MA10 indices. There does exist, however, a significant daily correlations for the MA3, MA4 and MA11 indices. This general characteristic is present in both of the East and West Coast correlations.

## 7.3 Cross Correlations of East and West Coast MA Indices

In processing the MA indices from two different sites, another important item of information is the extent of the cross correlation between the indices at the two sites. The cross correlation indicates the extent of the linear dependence between the data generated at one site with those generated at another site at a later time. One can calculate the cross correlation of the same MA indices between the two sites, for example, MA6 at Grafton with MA6 at Corralitos, or one can inter-mix the MA indices, for example, MA6 at Grafton with MA5 at Corralitos.

In this section we present results when the *same* MA indices are cross correlated between the two sites. The mathematics here is an extension of that of the autocorrelation estimates presented earlier. Inter-mixing of MA indices between the two sites is not treated in this report.

An estimate of the cross correlation at lag $k$, $\hat{R}_{C\,G}(k)$ can be represented mathematically as follows. We first define the estimate of cross covariance function at lag $k$, $\hat{K}_{C\,G}(k)$, as

$$\hat{K}_{C\,G}(k) = \frac{1}{N} \sum_{i=0}^{(N-1)-k} (M_C(i+k) - \overline{M_C})(M_G(i) - \overline{M_G}) \tag{10}$$

where $N$ is the number of data points, $M_C$ can be one of MA0,...,MA11 indices at Corralitos, $M_G$ can be one of MA0,...,MA11 indices at Grafton, $\overline{M_C}$ is the mean of the Corralitos data and $\overline{M_G}$ is the mean of the Grafton data. Note that the correlation lag $k$ can vary from 0 up to and including lag $N-1$.

The cross correlation is then the normalized cross covariance and is given by

$$\hat{R}_{C\,G}(k) = \frac{\hat{K}_{C\,G}(k)}{\sqrt{\hat{K}_{C\,C}(0)}\sqrt{\hat{K}_{G\,G}(0)}} \tag{11}$$

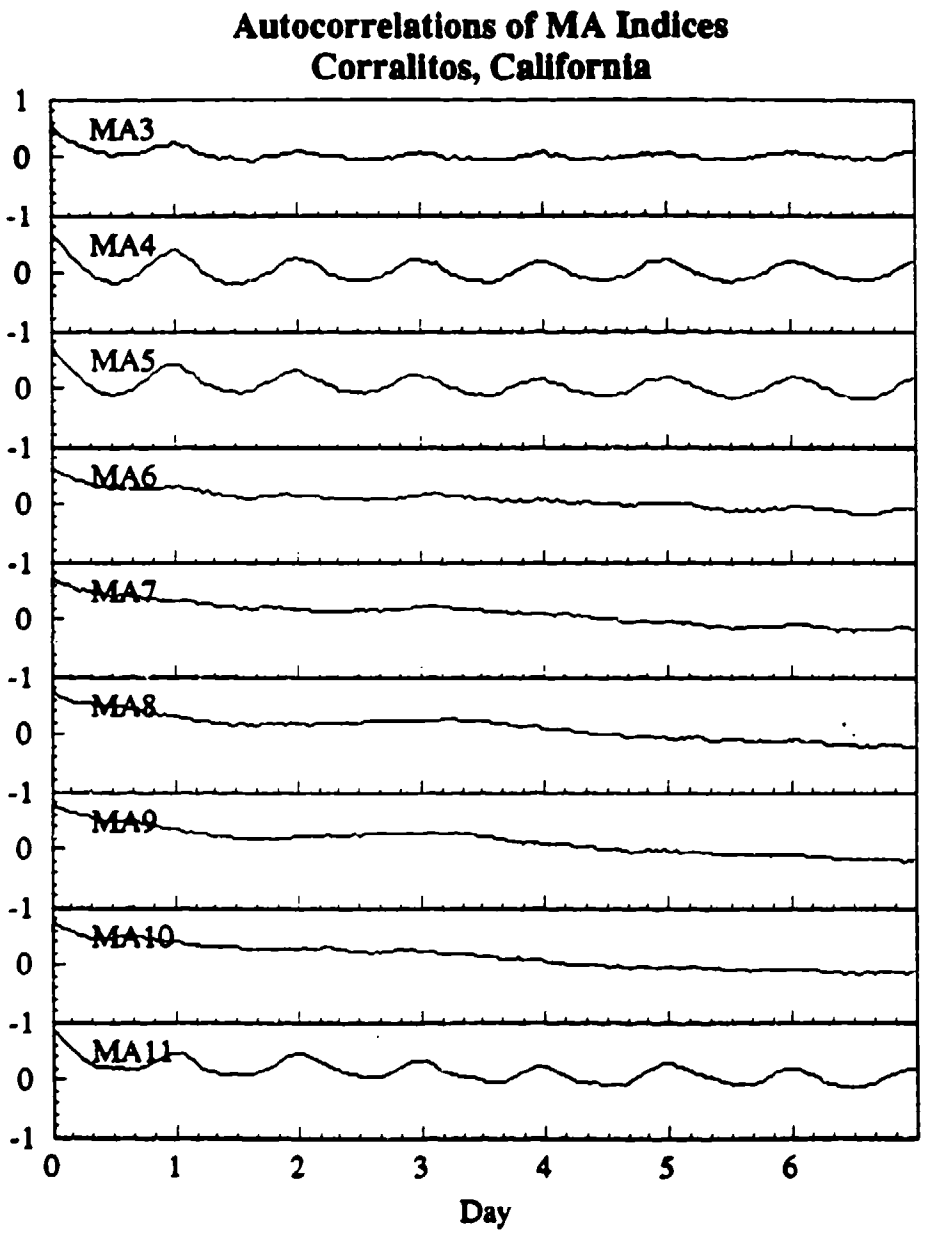


Figure 14: Nine plots showing the autocorrelations of MA indices MA3 through MA11 generated at Corralitos.

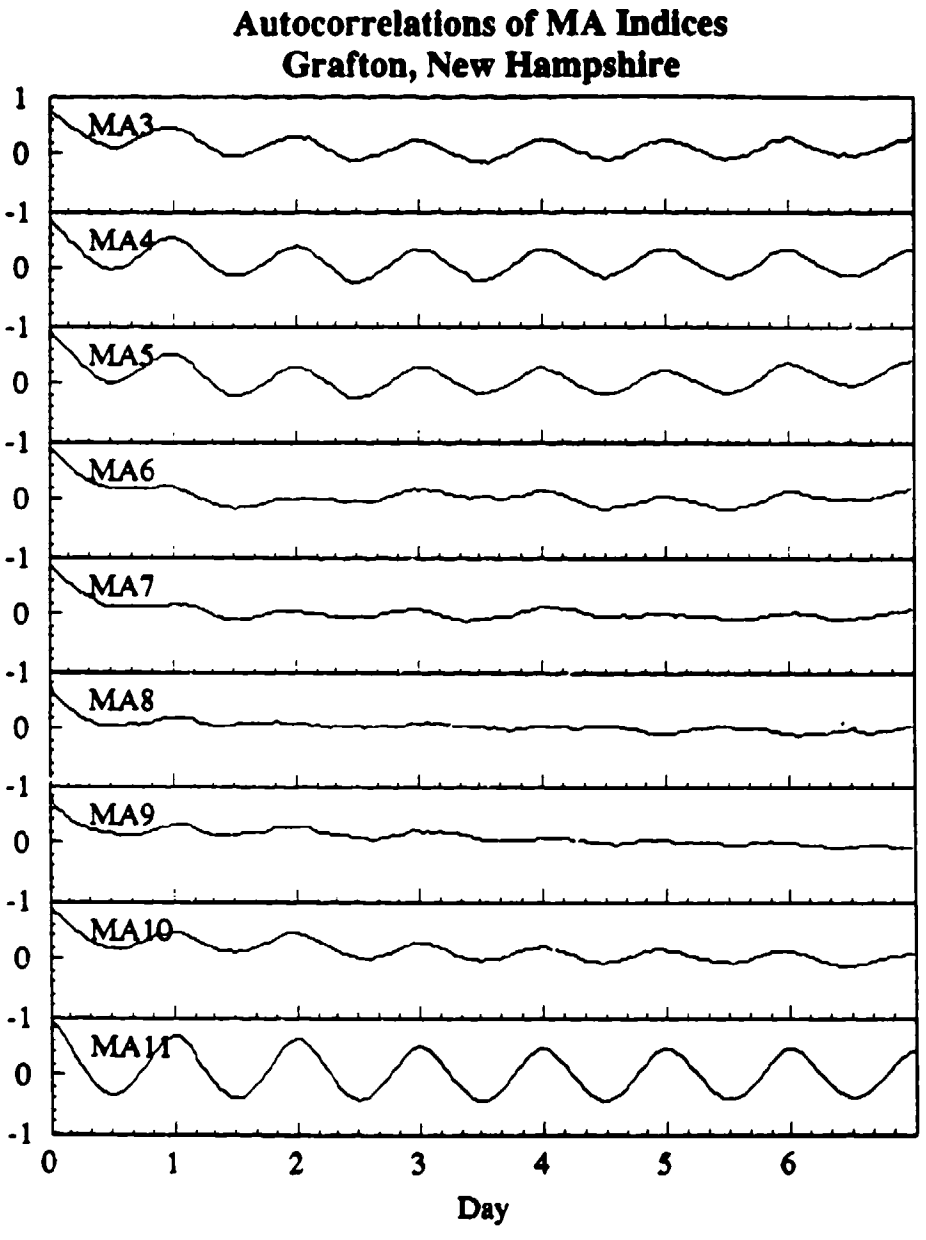


Figure 15: Nine plots showing the autocorrelations of the MA indices MA3 through MA11 generated at Grafton.

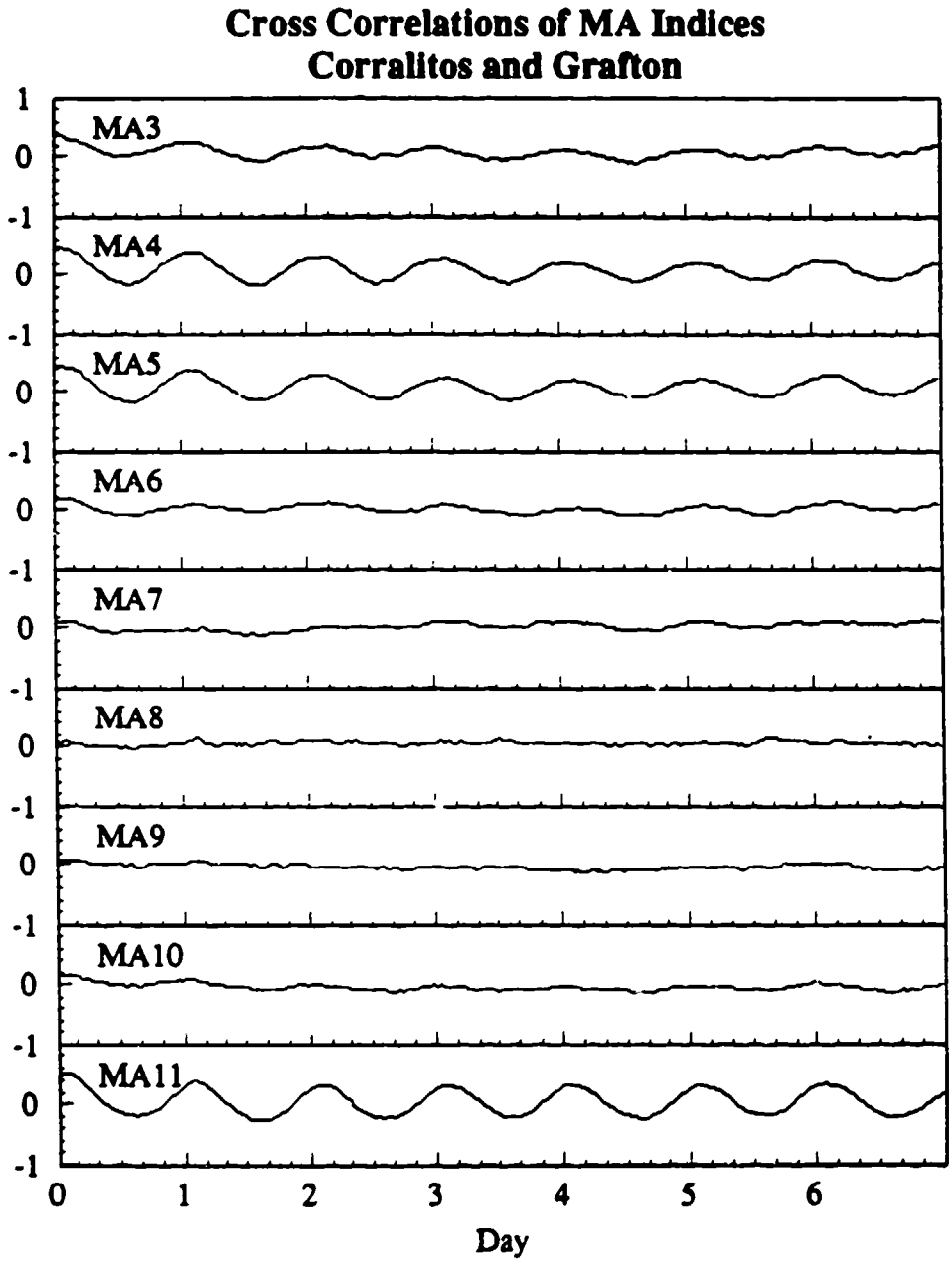


Figure 16: Nine plots showing the cross correlations of the MA indices MA3 through MA11 generated at Corralitos and Grafton.

The cross correlations between the nine MA indices for the Corralitos and Grafton sites for lags of up to a week are shown in Figure 16. These were calculated using the data from the month of January, 1988, at each location.

The cross correlation plots repeat the characteristics seen in the individual autocorrelation plots of the Grafton and Corralitos data. The MA6, MA7, MA8, MA9 and MA10 indices again tend to have weak cross correlations, and the remaining MA indices have some daily cross correlations.

One would expect a peak in the cross correlation plots at lags of about 3 hours since Corralitos geographically lags Grafton in time by approximately 3 hours. Looking closely at the plots, one can see that MA11 cross correlation has a peak that occurs at lags of 1.5 to 2 hours (not 3 hours), and that most of the remaining MA indices do not have any peaks during the first 3 hours. By analyzing another data set we have found the lags to be indeed approximately 3 hours, and so we attribute the inconsistencies in the plots to statistical fluctuations. Further work needs to be done to understand the reason for the lack of significant cross correlation peaks in some of the bands.

# 8 MAD-Specific MA Indices

The MA indices MA0, MA1, and MA2 cover frequency bands that are overlapping subsets of the other nine MA indices. As described earlier (see Section 2) the frequency ranges of the MA0, MA1 and MA2 indices were chosen to correspond to typical settings of the MAD equipment used by the U.S. Navy. These three MA indices allow one to study the characteristics of the magnetic activity in bands of specific interest to the Navy.

The MA0, MA1 and MA2 indices generated at Grafton, New Hampshire, during the week of November 9, 1987, are plotted in Figure 17. The general characteristics of the plots in Figure 11 are repeated. However, the new plots show a remarkable dynamic change of the power of the magnetic activity in the MA1 frequency band over a rather short period of time. The smallest value reached by the MA1 index on November 12, 1987 is 2.21, and the largest value of the MA1 index reached on November 13, 1987 is 15.72. This change of MA1 index occurs within a time frame of approximately one and a half day. One can translate the MA index values to dB values, since each unit increment of the MA index corresponds to a doubling of the power present in the corresponding frequency band. Thus, each MA index unit step is equivalent to $10 \log 2.0 = 3.01$ dB. Therefore, the increase of the magnetic activity in the MA1 frequency band is equivalent to an increase of $(15.72 - 2.21) \times (3.01) = 40.67$ dB. This is a large increase and since such large increases do not appear to be uncommon, it has important implications for MAD operations.

An event which could strongly influence the levels of geomagnetic activity is a solar flare. This can clearly be seen by examining the MA indices during a solar flare. The MA Index Generation System at Grafton was operating during the time of a

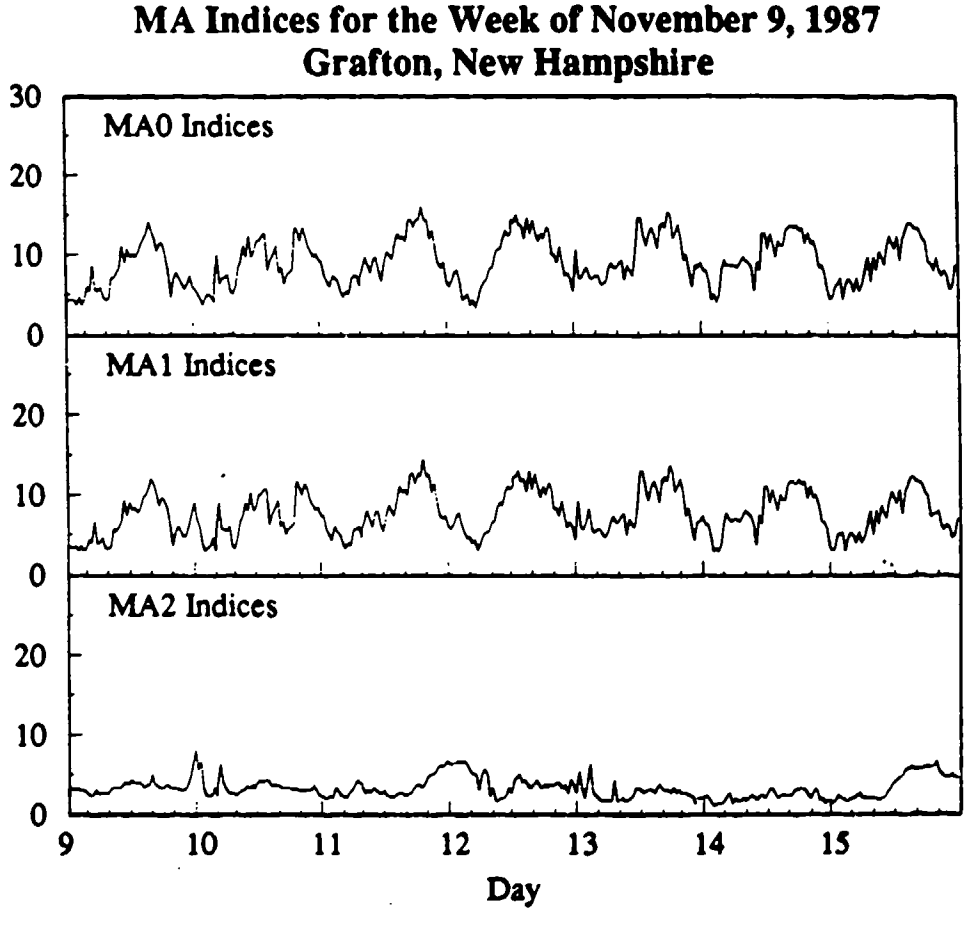


Figure 17: MA0, MA1 and MA2 indices generated at Grafton, New Hampshire for the week of November 9, 1987.

comparatively large solar flare that occurred during the last week of June 1988 (Optical Importance of 2B). There is a tremendous change in the character of the magnetic activity in all of the MA bands. Figure 18 shows the nine MA indices covering the frequency range from 0.01 to 10.0 Hz. We would like to emphasize that these are preliminary plots, and that their accuracies remain to be verified. The California MA Index Generation System was not operating during this period of time, and thus independent verification of these results is not possible. Note the large levels of magnetic activity that begin on the 23rd day of June. There is a clear 'quiet' geomagnetic time during the 24th and first half of the 25th of June, followed by large activity on the 26th and 27th of the month. The magnitudes of the power of geomagnetic activity during the two active times are relatively similar, and in both cases the upper limits of the dynamic range of the MA Index Generation System were reached.

The reasons for the presence of a quiet time in between the two storms is not clearly understood, and further work needs to be done to study its significance. An interesting point concerning the quiet period is that the level of the MA indices during that time is lower than the lowest levels of the MA indices that is normally present. This feature is most obvious in the higher MA bands.

In Figure 19 we plot the MA indices that are specifically chosen for the MAD operations, for the week of the solar flare. In addition, the $Kp$ indices for the same week are plotted. We can immediately notice that the $Kp$ indices do not represent the extent of the magnetic activity that was present in the MAD bands of interest. In fact the $Kp$ indices indicate quiet magnetic activity on the 23rd of June, whereas the MA indices all indicate large powers for the magnetic activity in their respective frequency bands. Clearly the use of $Kp$ indices can be misleading when one is interested in the levels of the power of the geomagnetic signals.

We can look at the MA0 band to see the range of variation of the power of the magnetic signals during the solar flare. The lowest level of the MA0 indices reached on the 24th was 3.55, and the highest level was 20.16 on the 26th. Following a similar calculation as that done at the beginning of this section we see that the magnetic activity has varied by approximately 50 dB in two days. This range is larger than the linear dynamic range of the MA Index Generation Systems, and the system at Grafton had recorded warning messages indicating many instances of saturated signal levels during that period.

The above calculations show the desirability of having up-to-date information of the magnitude of the naturally occurring magnetic activity when MAD equipment is being operated.

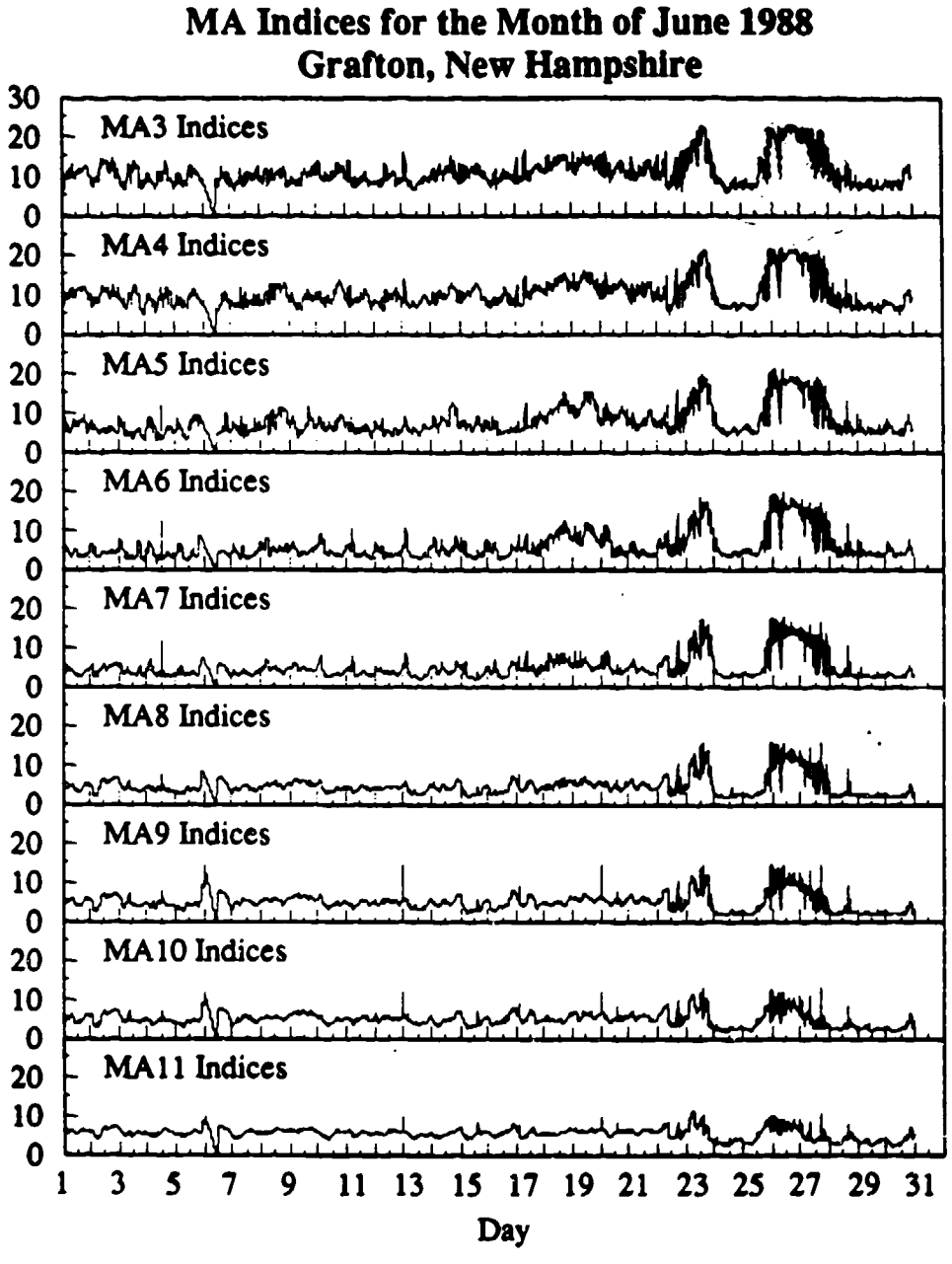


Figure 18: Plots of nine MA indices generated at Grafton, New Hampshire for the month of June 1988.

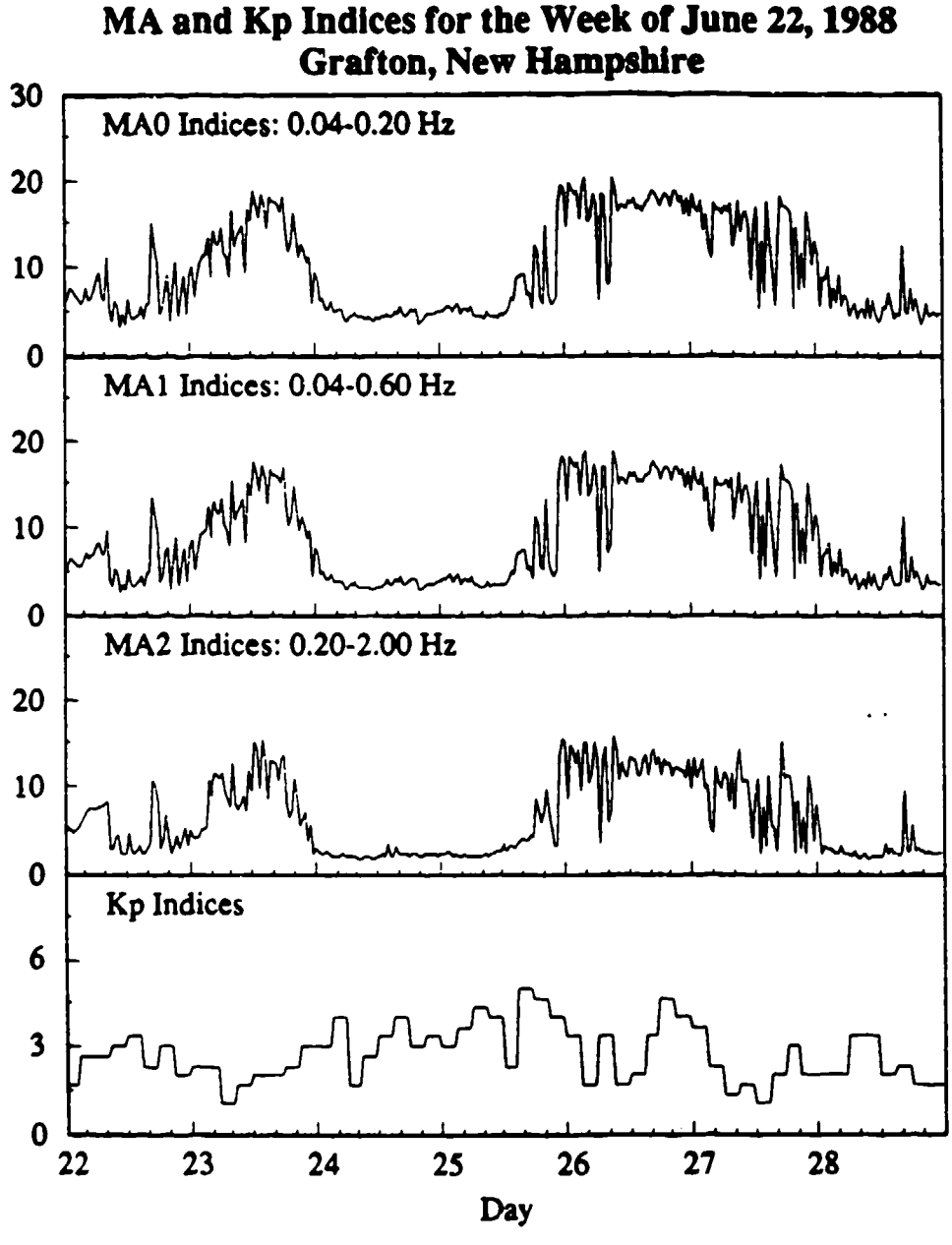


Figure 19: MA0, MA1 and MA2 indices generated at Grafton, New Hampshire, for the week of June 22, 1988, and the corresponding $Kp$ indices.

# 9 Predictions of MA Indices

The autocorrelation analysis of the MA indices in Section 7.2 demonstrated the linear dependencies that exist between a MA index and the same MA index at a later time. This information can be used to provide predictions of the MA indices for various lead times. The procedure is to use the autocorrelation time dependencies to obtain a prediction that is consistent with both the already observed data, and the autocorrelation measurements.

The prediction technique is usually referred to as Linear Prediction (LP) in engineering, or Autoregressive (AR) modeling of time series in statistics. The idea behind the technique is rather simple: the time series is modeled by an autoregressive filter driven by white noise. The unknown parameters are therefore the white noise and the filter itself. Thus, the time series at time $n$, $y(n)$, is assumed to be the output of a filter such that it depends linearly on the previously observed data, added to some random white noise, *i.e.*

$$y(n) = a_1 y(n-1) + a_2 y(n-2) + \cdots + a_p y(n-p) + z(n) \tag{12}$$

where the filter has order $p$ and the white noise at time $n$ is $z(n)$. These topics are disussed in detail, for example, by *Makhoul* [1975], *Box and Jenkins* [1976], and by *Priestly* [1984].

To model the data successfully one needs to obtain reasonable estimates of the model parameters $a_1, \ldots, a_p$. The esimates will be referred to as $\hat{a}_1, \ldots, \hat{a}_p$. These are obtained by minimizing the mean square error between the observed value at time $n$ and the predicted value for time $n$. The one step prediction for time $n$ is given by

$$\hat{y}(n) = \hat{a}_1 y(n-1) + \hat{a}_2 y(n-2) + \cdots + \hat{a}_p y(n-p) \tag{13}$$

and thus the prediction error at time $n$ is

$$e(n) = \hat{y}(n) - y(n). \tag{14}$$

By minimizing $e(n)^2$ one can obtain estimates of the true filter parameters $a_1, \ldots, a_p$. The minimization is done over the set of already observed $y(.)$ data. The minimization leads to a set of $p$ simultaneous equations in $p$ unknowns that can be efficiently solved in a recursive manner [*Levinson*, 1947; *Durbin*, 1960]. The selection of the proper order of the filter is an additional complication in applying the above procedure. Various techniques are available for deciding on the order of the predictor filter, the most widely used one being due to *Akaike* [1969, 1974].

The linear prediction technique was applied to the MA indices to see its effectiveness. One week of data from Grafton (starting November 9, 1987), and one week from Corralitos (starting November 20, 1987) was processed. In both cases the MA5 indices were predicted for lead times of $1/2, 1, 2, 4, 8, 12, 18, 24$ hours. A 96-th order filter was used for the predictions, and the estimates of the AR parameters of the filters were

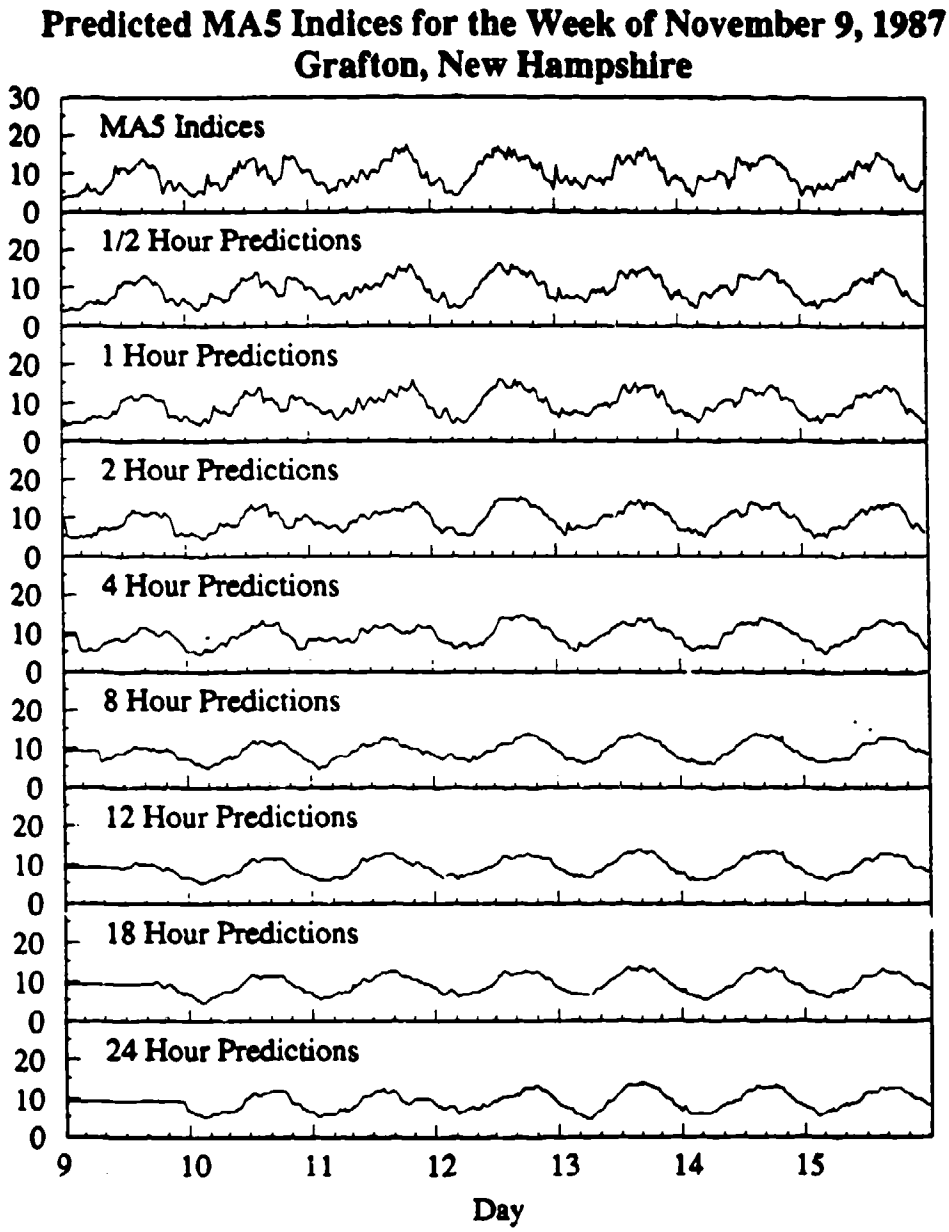


Figure 20: Nine plots showing the MA5 indices (top plot) of Grafton, New Hampshire, and predictions of the MA5 indices for various lead times.

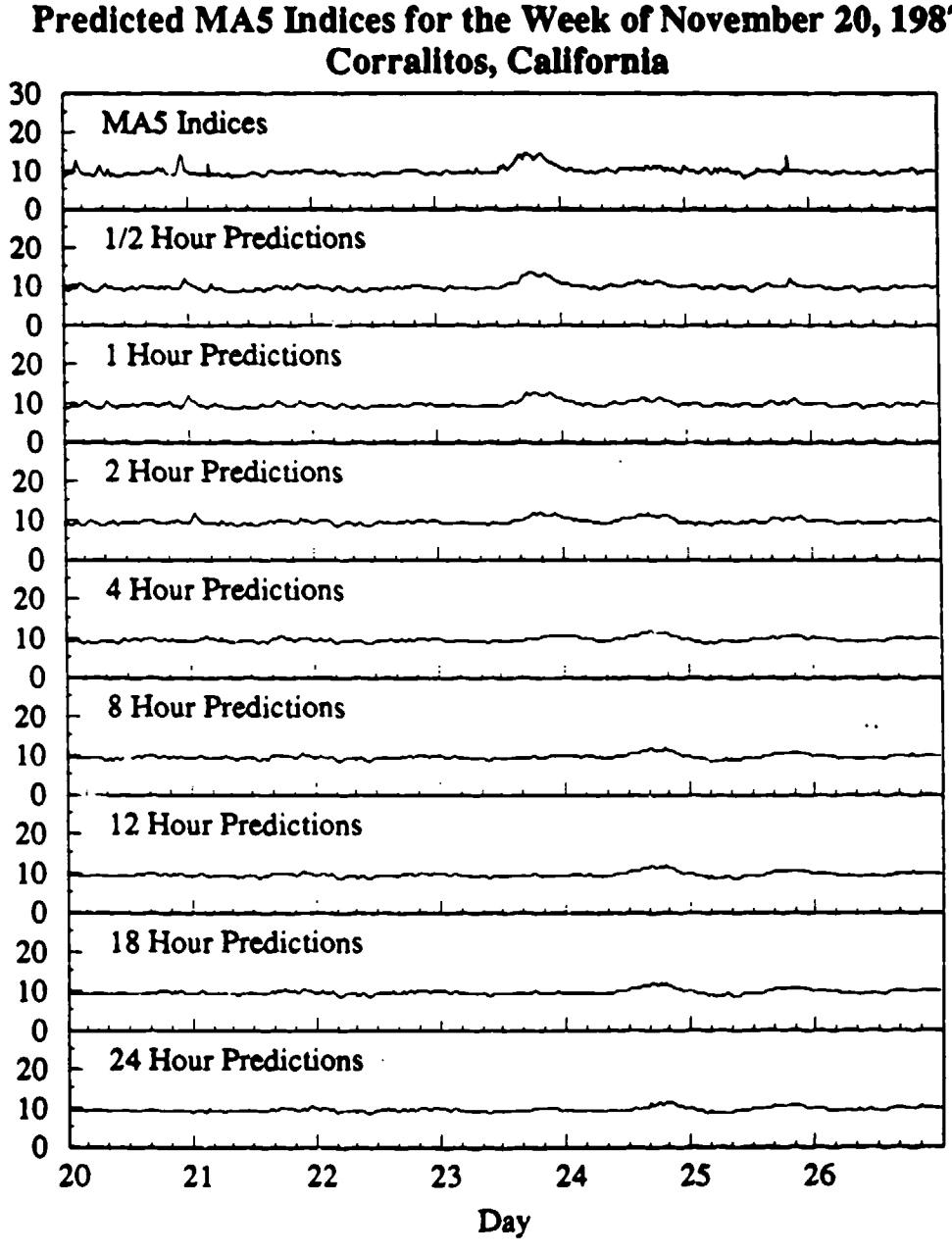


Figure 21: Nine plots showing the MA5 indices (top plot) of Corralitos, California, and predictions of the MA5 indices for various lead times.

Table 6: Percent errors of the predictions of MA5 indices for Grafton and Corralitos. The Grafton data are predicted well for all the lead times since the actual measured data match the autocorrelations expected from analysis of the previous month.

| Lead Time in Hours | Percent Error in Predictions for Grafton (Figure 20) | Percent Error in Predictions for Corralitos (Figure 21) |
|---|---|---|
| 1/2 | 18.6 | 42.5 |
| 1 | 27.1 | 54.4 |
| 2 | 36.2 | 68.5 |
| 4 | 45.9 | 82.6 |
| 8 | 48.0 | 99.5 |
| 12 | 43.0 | 99.8 |
| 18 | 41.7 | 99.3 |
| 24 | 51.7 | 95.4 |

obtained by minimizing the square of the one step prediction error over the previous one month of observed MA5 indices. Once the prediction filters were calculated for each site, they were used to predict the MA5 indices for the week of data under study. The resulting predictions are shown in Figures 20 and 21.

In Figure 20 one can see that the 1/2 hourly predictions tend to be the most accurate. This is because the prediction filter begins to respond immediately to any changes that occur in the data. For example, a sudden peak of the data is followed by 1/2 hourly predictions with high values. However, as the lead time of the predictions is increased, the currently observed data become less correlated with the values that are to be predicted. Thus the prediction error tends to increase, as one may expect, as the lead time of the predictions is increased. For example, the 24 hourly predictions seem to capture only the overall daily variations present in the MA5 index.

The second set of predictions correspond to a very different set of data, which was chosen as a worst case scenario. The MA5 indices obtained at Corralitos for the week of November 20, 1987, do not have any of the diurnal variations seen in Grafton. There is only a one day peak of the MA5 indices present on the 23rd of the month. Again the 1/2 hourly predictions are seen to match the data. However, as the lead time of the predictions increases to 24 hours, the linear predictor has difficulty predicting the MA5 peak on the 23rd of the month. In fact, there is a delay of about one day before the effect of the peak is propagated within the prediction mechanism, and the predictor attempts to predict large values on the 24th of the month.

These examples demonstrate both the effectiveness of the linear prediction technique when high autocorrelations of the indices are present, and its weaknesses when the technique tries to predict sudden changes of the MA indices that differ from the

autocorrelation data. In general, the MA indices that cover the low frequency bands have high autocorrelation values even for lags of 24 hours. Consequently one would expect to be able to provide reasonable predictions of up to 24 hours ahead, except for sudden bursts of geomagnetic activity.

Table 6 lists the percentage errors for the predictions of the Grafton and Corralitos MA5 indices. The percentage errors are calculated by dividing the square error of the predictions by the power of the MA5 indices (with the means removed). It is seen that the percentage error of the predictions for both sites tends to increase as the lead time of the predictions increases. The Grafton MA5 indices are better predicted since they match the autocorrelation profiles of the the indices calculated from the preceding days. However, the Corralitos MA5 indices do not match their expected autocorrelation profiles, and so are predicted with less success.

# 10 Conclusions and Future Research

We have described a digital remote monitoring system for the study of magnetic activity in the 0.01 Hz to 10 Hz range. Two of the systems have been successfully operated on the East and West coasts of the U.S., but a longer term deployment of these systems would be needed in order for the usefulness of their indices to be checked operationally. In addition, a long term statistical study of the MA indices would enable us to make reliable estimates of the types of activity that occur in these frequency bands. We have already observed daily variations, but monthly and seasonal variations should also be expected.

In this report, the MA indices obtained at these sites have been processed to obtain initial estimates of the types of relations between the indices at the same site, and between the indices at different sites. The information thus gathered has enabled us to predict the MA indices for up to a day ahead, and we have shown the quality of our predictions to be moderately good.

For MAD equipment operating in the 0.04 to 2.0 Hz frequency range, the MA indices provide an indication of the average power of the background magnetic activity. We have compared the MA indices with the standard $Kp$ indices and have found them to have very different characteristics. We feel that the information on the average power of the geomagnetic activity, which is not available through the $K$ indices, would be helpful in the MAD operations, since it would provide the operators with information about the actual and expected natural noise levels in the MAD band.

Future research could follow several different paths. The first path that can be taken is improvements to the signal processing techniques. There have been many recent advances in linear prediction theory, especially in multi-channel applications. These results can be applied for prediction and for modeling of the processes that generate the magnetic activity in the MA frequency bands. Data from other measurements, such as sunspot numbers, $Kp$ indices, and other MA indices can be incorporated into the prediction mechanisms that have already been studied. One would expect to be

able to improve the prediction quality of the various MA indices by incorporating the additional information.

Maximum entropy techniques can be used to account for uncertainties in the measurements of the various autocorrelation and cross correlation values, improving the modeling of the MA indices with autoregressive processes. This allows one to make the calculated model less dependent on the specific 'training set' of MA indices used, thus obtaining a more general linear description of the MA indices. These linear models can then be used, for example, to study the stationarity of the MA indices, since one would expect them to be stationary over the short term, but maybe not so in the long term. The length of time of the expected short term stationarity is not known.

A second path of research would be the construction of other MAI Generation Systems, and their operation at various selected geographic sites. The hardware cost of each of these stations is relatively small. The simultaneous availability of MA indices from a number of locations would give important information about the geographic variation of the indices. Measurements at higher geomagnetic latitudes appear particularly important, because of the likely high levels of noise in the MAD band. Knowing the geographical scale of these pulsation events would allow the MAD operations at locations *within range* of a specific site to be more successful, by using the MA indices to decide the settings of their MAD equipment.

Finally, the present MAI Generation System can be improved in several aspects. First, it would be informative if more spectral information could be stored, instead of just the 12 MA bands. A possible change that would accomplish this is the addition of a larger data storage device. Second, the MA indices could be evaluated more often, for example, every 15 minutes. Additional research should be done to justify the statistical reliability of the spectral estimates if shorter times are considered. Other types of information could be analyzed in addition to the spectral information. Maximum and minimum values of the magnetic activity during a half hour period could be recorded, or, to obtain even more detail, half hourly histograms of the distribution of the magnetic activity observed at a site could be computed. These additional data would enable the types of magnetic activity that occur in the 0.01 Hz to 10 Hz frequency range to be better described by our indices.

# References


Akaike, H., Fitting autoregressive models for prediction, *Ann. Inst. Statist. Math., 21*, 243-247, 1969.

Akaike, H., A new look at the statistical model identification, *IEEE Trans. Autom. Control, 19*, 716-723, 1974. Reprinted in *Childers* [1978].

Bernardi A., A.C. Fraser-Smith, and O.G. Viilard, Jr., *A real time index of geomagnetic background noise for the M.A.D. frequency range*, Tech. Rept. No E724-1, Space, Telecommunication and Radioscience Laboratory, Stanford University, Stanford, CA, 1985.

Box, G.E., and G.M. Jenkins, *Time Series Analysis Forecasting and Control*, Holden-Day, Oakland, California, 1976.

Childers, D.G., ed., *Modern Spectrum Analysis*, IEEE, New York, 1978.

Durbin, J., The fitting of time-series models, *Rev. Int. Inst. Statist., 28*, 233-243, 1960.

Fraser, B.J., Polarization of Pc 1 pulsations at high and middle latitudes, *J. Geophys. Res., 80*, 2797-2807, 1975.

Fraser-Smith, A.C., and D.B. Coates, Large amplitude ULF electromagnetic fields from BART, *Radio Sci., 13*, 661-668, 1978.

Grossner, N.R., *Transformers for Electronic Circuits*, McGraw-Hill, New York, 1983.

Ho, A.M.-H., A.C. Fraser-Smith, and O.G. Villard, Jr., Large-amplitude ULF magnetic fields produced by a rapid transit system: Close-range measurements, *Radio Sci., 14*, 1011-1015, 1979.

Jacobs, J.A., *Geomagnetic Micropulsations*, Springer, New York, 1970.

Joselyn, J.A., A Real-Time Index of Geomagnetic Activity, *J. Geophys. Res., 75*, 2777-2780, 1970.

Levinson, H., The Wiener RMS (root mean square) error criterion in filter design and prediction, *J. Math. Phys., 25*, 261-278, 1947.

Lincoln, J.V., Geomagnetic Indices, pp. 67-100 in *Physics of Geomagnetic Phenomena*, Vol. 1, Ed. S. Matsushita and W.H. Campbell, Academic Press, New York, 1967.

Makhoul, J., Linear prediction: A tutorial review, *Proc. IEEE, 63*, 561-580, 1975. Reprinted in *Childers* [1978].

Patubo, P., BART Public Affairs Office, personal communication, 1986.

Priestley, M.B., *Spectral Analysis and Time Series*. Academic Press, London, 1984.

Prochaska, R.D., Geomagnetic Index Calculation and use at AFGWC, Report No. AD A088234, HQ Air Force Global Weather Central (MAC), Offutt AFB, NB, 1980.

Rostoker, G., Geomagnetic Indices, *Rev. Geophys. Space Phys., 10*, 935-950, 1972.

Sentman D.D., PC Monitors Lightning Worldwide, *Computers in Science, 1*, 25-34, 1987.

Samadani, R., A.C. Fraser-Smith, and O.G. Villard, Jr., Possible changes in natural Pc 1 pulsation activity caused by BART, *J. Geophys. Res., 86*, 9211-9214, 1981.

Welch, P.D. The use of fast Fourier transform for the estimation of power spectra: A method based on time averaging over short, modified periodograms, *IEEE Trans. Audio and Electroacoust., 15*, 70-73, 1967. Reprinted in *Childers* [1978].

DISTRIBUTION LIST

| Organization | Copies |
|---|---|
| Defense Advanced Research Projects Agency<br>ATTN: STO, D.C. Lewis<br>1400 Wilson Blvd<br>Arlington, VA 22209 | 1 |
| Defense Nuclear Agency/RAAE<br>ATTN: CAPT J. Emmes<br>L. Wittwer<br>Washington, D.C. 20305 | 1<br>1 |
| Defense Technical Information Center<br>Bldg 5, Cameron Station<br>Alexandria, VA 22314 | 12 |
| Department of the Air Force<br>Air Force Geophysics Laboratory<br>ATTN: P. Kossey<br>J. Rasmussen<br>Hanscom AFB, MA 01731 | 1<br>1 |
| Department of the Air Force<br>Rome Air Development Center/EEPS<br>ATTN: J. Turtle<br>Hanscom AFB, MA 01731 | 1 |
| Department of the Navy<br>Assistant Chief of Naval Operations (Air Warfare): NOP-503<br>ATTN: CAPT J. Baker<br>Washington, D.C. 20350-2000 | 3 |
| Department of the Navy<br>Deputy Chief of Naval Operations (Air Warfare): NOP-05<br>ATTN: VADM R.F. Dunn<br>Washington, D.C. 20350-2000 | 1 |
| Department of the Navy<br>Deputy Chief of Naval Operations (Naval Warfare): NOP-07<br>ATTN: VADM J.R. Hogg<br>Washington, D.C. 20350-2000 | 1 |
| Department of the Navy<br>Space and Naval Warfare Systems Command, Code TD80<br>ATTN: RADM C.E. Dorman<br>Washington, D.C. 20363-5100 | 1 |
| Naval Academy<br>Weapons Systems Engineering Department<br>ATTN: Chairman<br>Annapolis, MD 21402 | 5 |
| Naval Air Systems Command<br>PDA-13<br>ATTN: RADM W.L. Vincent<br>Washington, D.C. 20361 | 1 |
| Naval Air Systems Command<br>ATTN: C.C. Hanna<br>Jefferson Plaza #1<br>1411 Jefferson Davis Hwy<br>Arlington, VA 22202 | 2 |
| Naval Coastal Systems Center<br>ATTN: D. Skinner<br>West Highway 98<br>Panama City, FL 32407 | 3 |
| Naval Intelligence Support Center<br>ATTN: G.D. Batts<br>W. Reese<br>4301 Suitland Rd<br>Washington, D.C. 20390 | 1<br>1 |
| Naval Ocean R & D Activity<br>ATTN: D.L. Durham<br>D.W. Handschumacher<br>K. Smits<br>NSTL Station<br>Bay St. Louis, MS 39522 | 1<br>1<br>1 |
| Naval Postgraduate School<br>Department of Physics and Chemistry<br>ATTN: O. Heinz<br>Monterey, CA 93940 | 1 |
| Naval Research Laboratory<br>ATTN: Code 2627<br>Washington, D.C. 20375 | 6 |
| Naval Underwater Systems Center<br>New London Laboratory<br>ATTN: P. Bannister<br>A. Bruno<br>New London, CT 06320 | 1<br>1 |

DISTRIBUTION LIST

| Organization | Copies |
|---|---|
| Naval Weapons Center<br>ATTN: R.J. Dinger<br>China Lake, CA 93555 | 1 |
| Office of the Assistant Secretary of Defense ($C^3I$)<br>ATTN: T.P. Quinn<br>Pentagon 3E160<br>Washington, D.C. 20301 | 1 |
| Office of Naval Research<br>ATTN: R. Gracen Joiner<br>J.G. Heacock<br>800 N. Quincy Street<br>Arlington, VA 22217 | 5<br>1 |
| Office of Naval Research<br>Stanford University<br>ATTN: Resident Representative<br>Stanford, CA 94305 | 1 |
| Office of Naval Technology<br>Director ASW/UT<br>ATTN: A.J. Faulstich<br>800 N. Quincy Street<br>Arlington, VA 22217 | 3 |
| Bell Laboratories<br>ATTN: L.J. Lanzerotti<br>600 Mountain Avenue<br>Murray Hill, NJ 07974 | 1 |
| International Business Machines<br>Systems Integration Division<br>ATTN: G. Dailey<br>9500 Godwin Drive<br>Manassas, VA 22110 | 1 |
| Johns Hopkins University<br>Applied Physics Laboratory<br>ATTN: L.W. Hart<br>T.A. Potemra<br>Johns Hopkins Road<br>Laurel, MD 20707 | 1<br>1 |
| NASA Headquarters<br>Space Plasma Physics Branch<br>ATTN: G. Parks<br>S. Shawhan<br>Washington, D.C. 20546 | 1<br>1 |
| National Science Foundation<br>Division of Polar Programs<br>ATTN: J. T. Lynch<br>1800 G Street, N.W.<br>Washington, D.C. 20550 | 1 |
| R. & D. Associates<br>ATTN: C. Greifinger<br>P.O. Box 9695<br>Marina del Rey, CA 90291 | 1 |
| Stanford University<br>STAR Laboratory<br>ATTN: P.M. Banks<br>K.J. Harker<br>R.A. Helliwell<br>O.G. Villard, Jr.<br>Stanford, CA 94305 | 1<br>1<br>1<br>1 |
| SRI International<br>Remote Measurements Laboratory<br>ATTN: D. Bubenik<br>333 Ravenswood Avenue<br>Menlo Park, CA 94025 | 1 |
| University of California at Los Angeles<br>Department of Geophysics and Space Physics<br>ATTN: R.L. McPherron<br>Los Angeles, CA 90024 | 1 |
| Utah State University<br>Center for Atmospheric and Space Sciences<br>ATTN: W.J. Raitt<br>Lund Hall, Rm 320C<br>Logan, UT 84322-3400 | 1 |
| University of Maryland<br>Institute for Physical Science and Technology<br>ATTN: T.J Rosenberg<br>College Park, MD 20742 | 1 |
| University of Texas, Austin<br>Geomagnetics and Electrical Geosciences Laboratory<br>ATTN: F.X. Bostick, Jr.<br>Austin, TX 78712 | 1 |